Supplemental Figures

Noël *et al*.

A

TIL densities in our BC patient cohort (n=168)

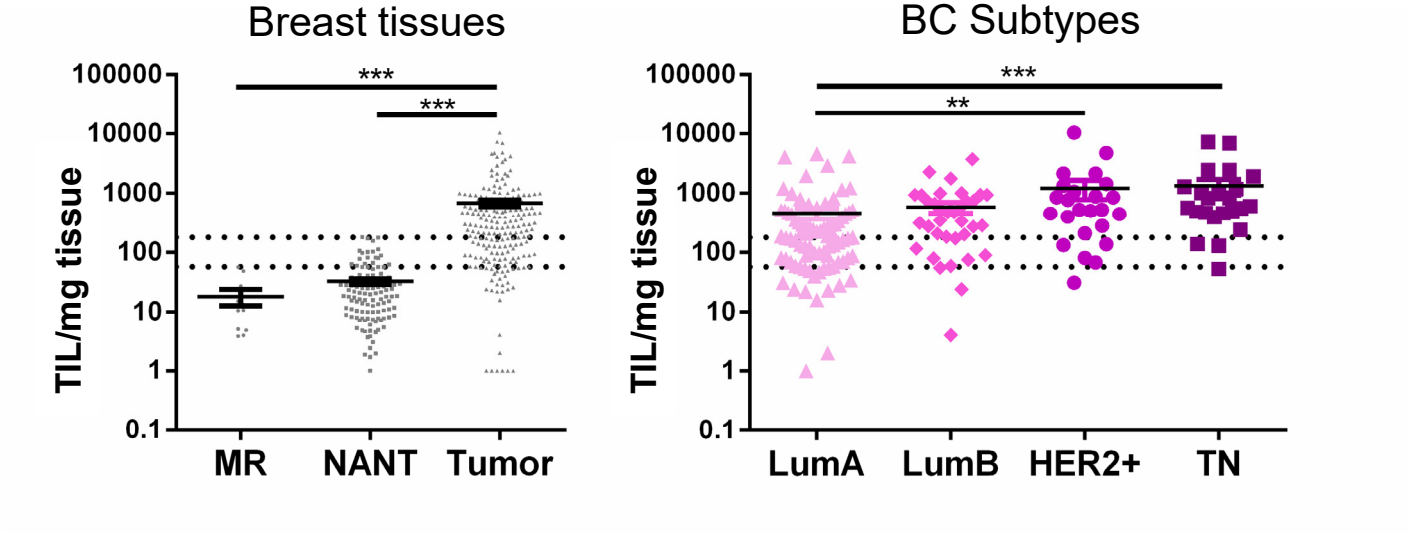

B

Flow cytometry gating strategies

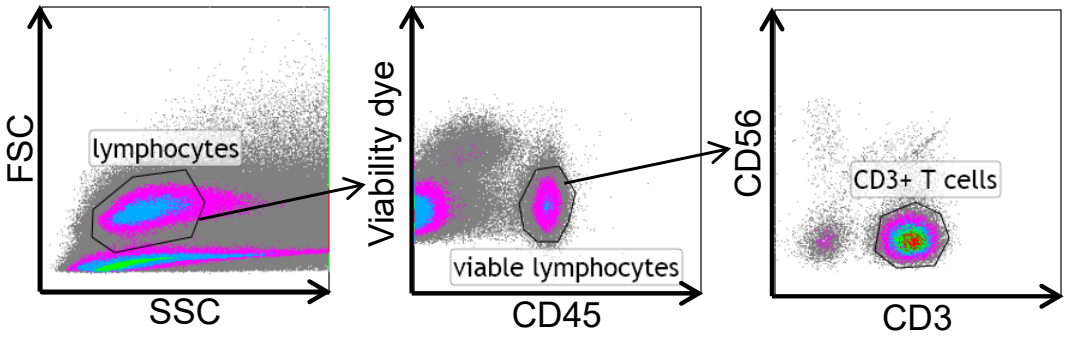

C

Correlation between BC CXCR5⁺ TIL subpopulation densities

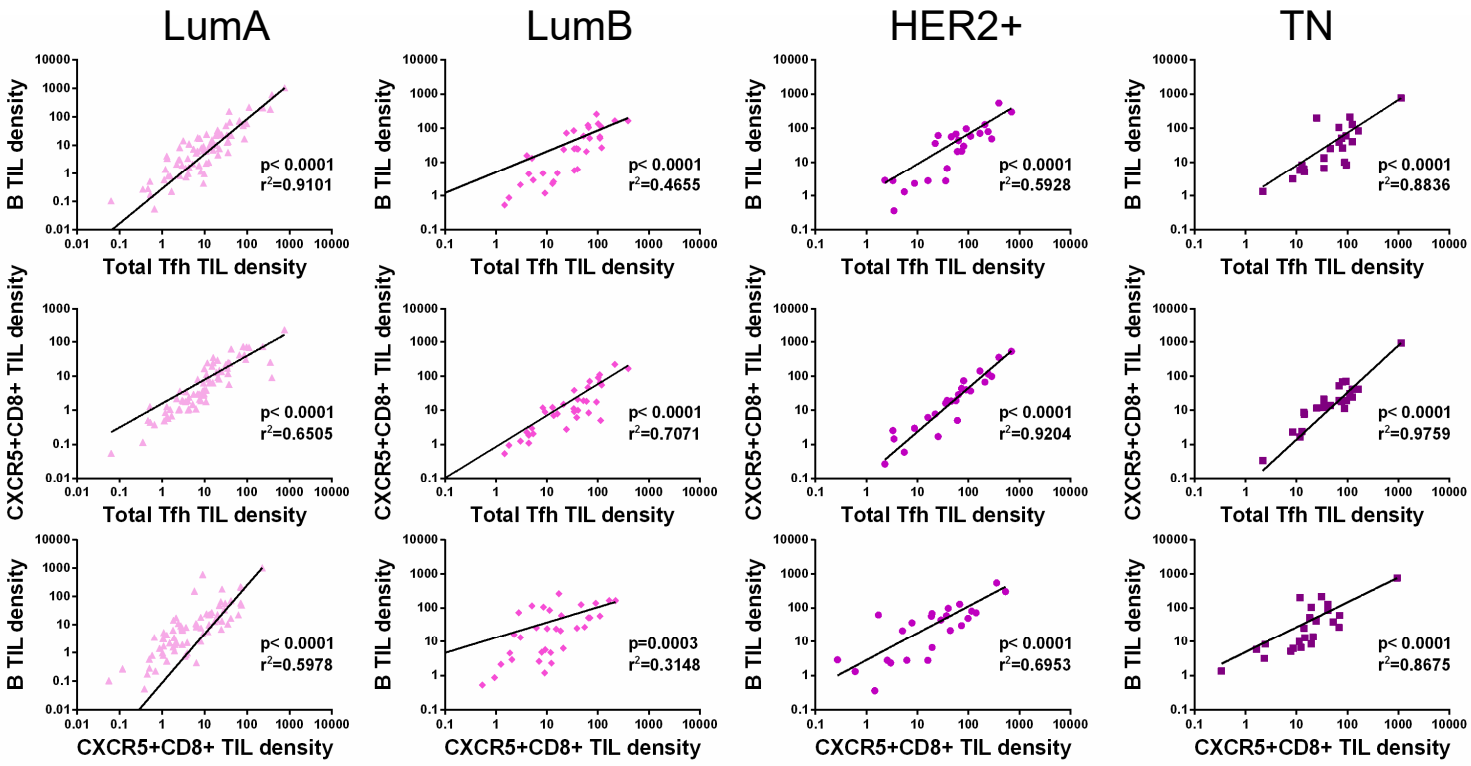

Human BC

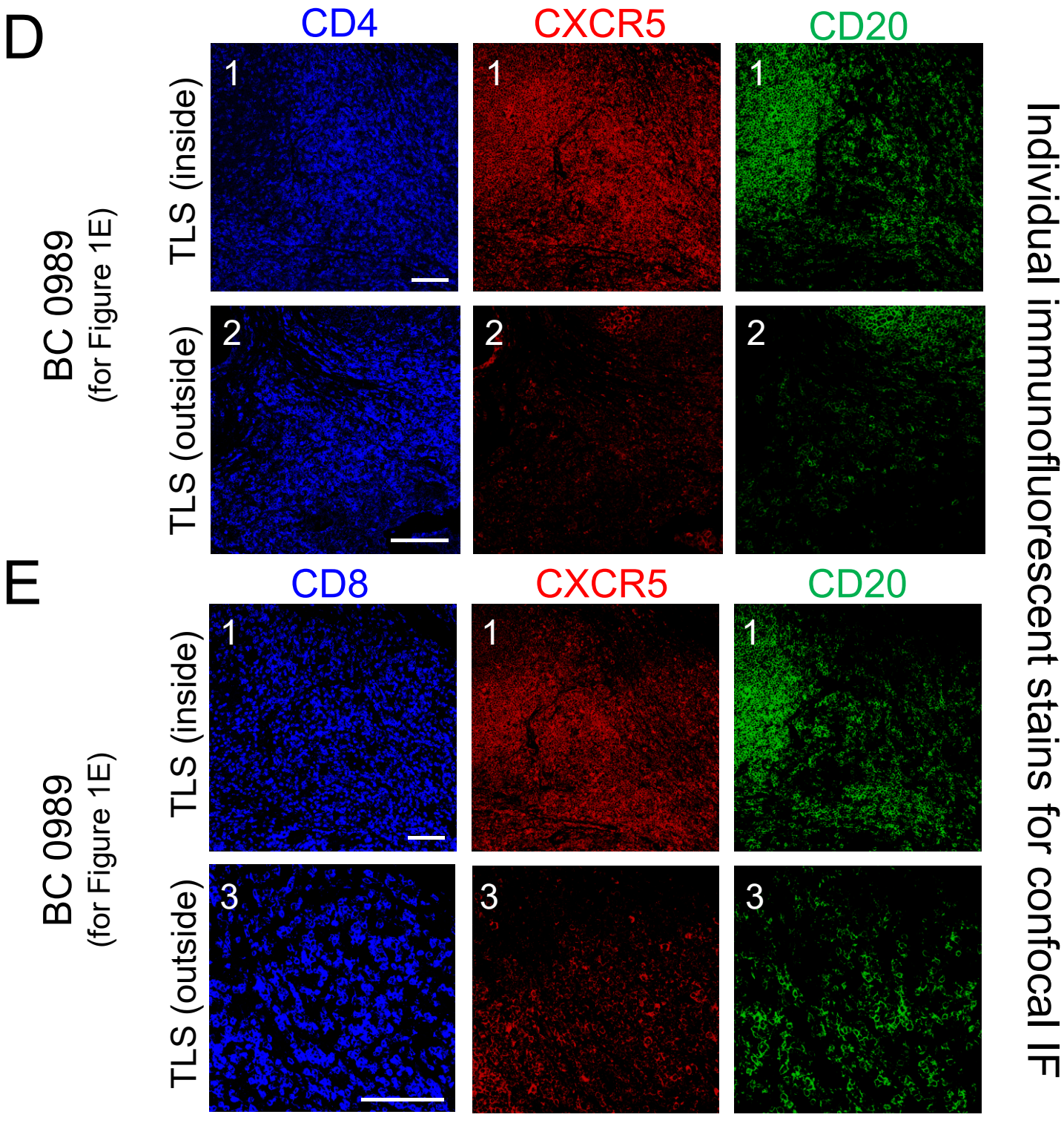
D
CD4
CXCR5
CD20
BC 0989
(for Figure 1E)
TLS (inside)
TLS (outside)
1
2
E
CD8
CXCR5
CD20
BC 0989
(for Figure 1E)
TLS (inside)
TLS (outside)
1
3
Individual immunofluorescent stains for confocal IF

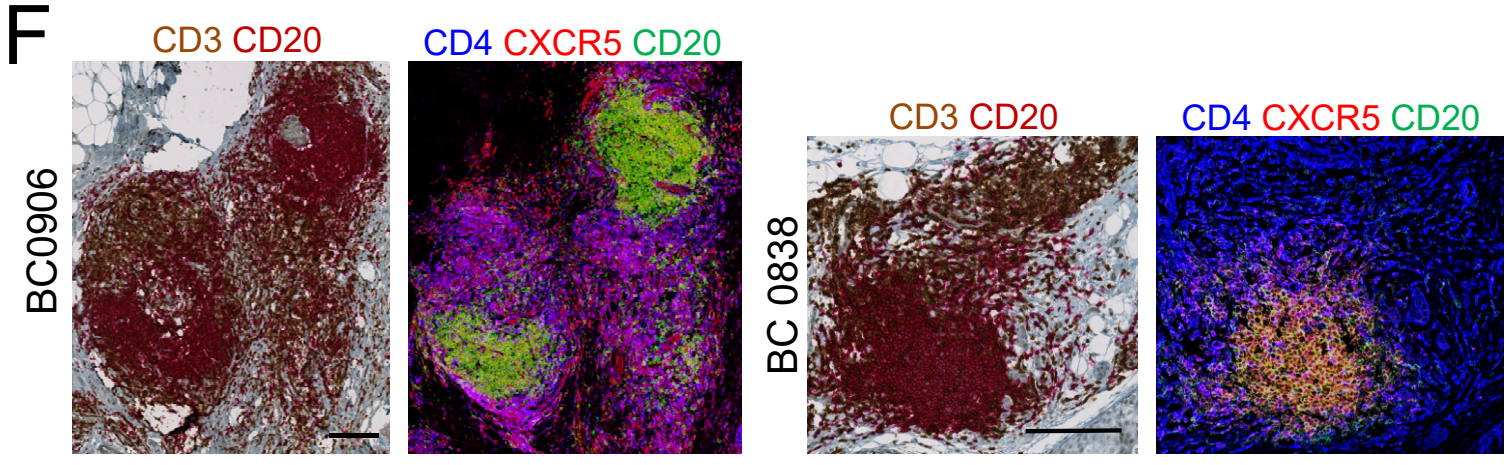
F
CD3 CD20
CD4 CXCR5 CD20
BC0906
CD3 CD20
CD4 CXCR5 CD20
BC 0838

Human BC

G

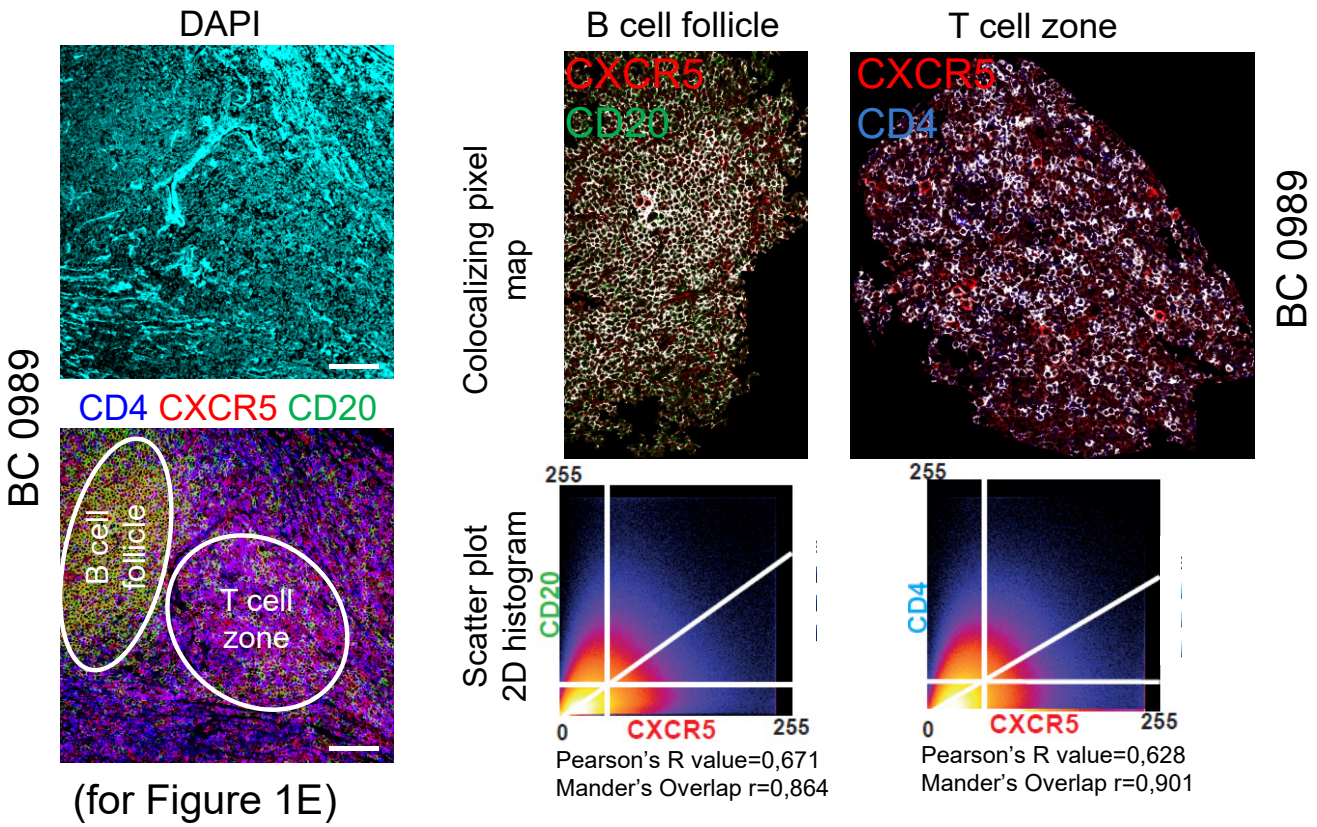

Human tonsil

H

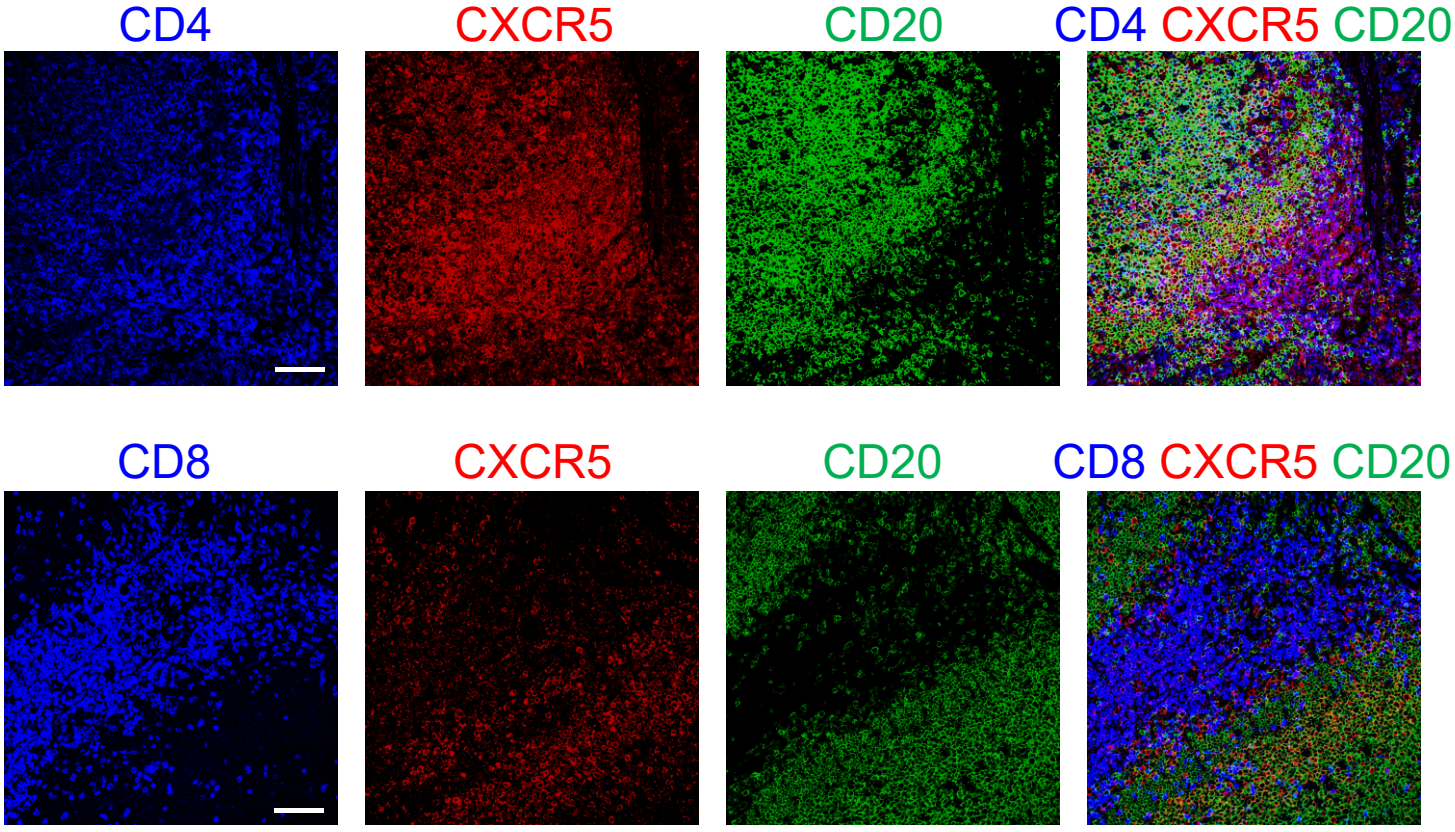

Supplemental Figure 1

A. TIL densities (the number of viable $CD45^+$ cells/mg of tumor tissue; flow cytometry) are shown for: *left graph*; different breast tissues including MR=mammary reduction (N=11), NANT=non-adjacent non-tumor tissue (N=115) and tumor (N=168)] or *right graph*: the BC subtypes Luminal A (LumA; N=82); Luminal B (LumB; N=36); HER2+ (N=24) and TN (N=26).

B. Example of the gating strategy used to analyze viable $CD45^+$ lymphocytes and $CD3^+$ T cells in human tonsils and breast tissue homogenates.

C. The densities (number of TIL/mg of tumor tissue) for total Tfh TIL ($CD4^+CXCR5^+$), TIL-B and $CD8^+CXCR5^+$ TIL are correlated with one another across the BC subtypes (LumA, N=82; LumB, N=36; HER2+, N=24; TN, N=26).

D and E. Individual IF stains for CD4 (**D)** or CD8 (**E)** (blue), CXCR5 (red) and CD20 (green) captured by confocal microscopy with the merged image shown in Figure 1F (BC 0989). White scale bars = 100μm.

F. Dual cIHC stainings for CD3 (brown)/CD20 (red) and confocal IF staining for CD4 (blue), CXCR5 (red), CD20 (green) on 2 consecutive FFPE tumor sections from 2 human BC tumors [a different region in the CD4/CXCR5/CD20 stain of BC 0906 is also shown in Figure 2C), TN, left panels and BC 0838, Lum A, right panels]. Black scale bars: 200μm.

G. For the TLS shown in Figure 1E (area 1): DAPI staining (*upper left panel*) and localization of the B cell follicle and T cell zone (*lower left panel*). White scale bars = 100μm. Pixel analysis to quantify CD20 and CXCR5 co-localization in the B cell follicle (*middle panels*) and CD4 and CXCR5 co-localization in the T cell zone (*right panels*). Co-localization analysis was performed using the JACOP Fiji plugin. *Upper panel:* shows the co-localized pixel map (white pixels) in the defined regions. *Lower panel:* shows a cytofluorogram for pixel intensity distribution. Pearson and Mander's coefficients are indicated under the image.

H. IF stains captured by confocal microscopy for CD4 (*upper panels*, blue) or CD8 (*lower panels*, blue) together with CXCR5 (red) and CD20 (green) on two FFPE tonsil sections. White scale bars = 100μm.

Supplemental Figure 2
Noël, *et al.*

A TIL in BC Subtypes

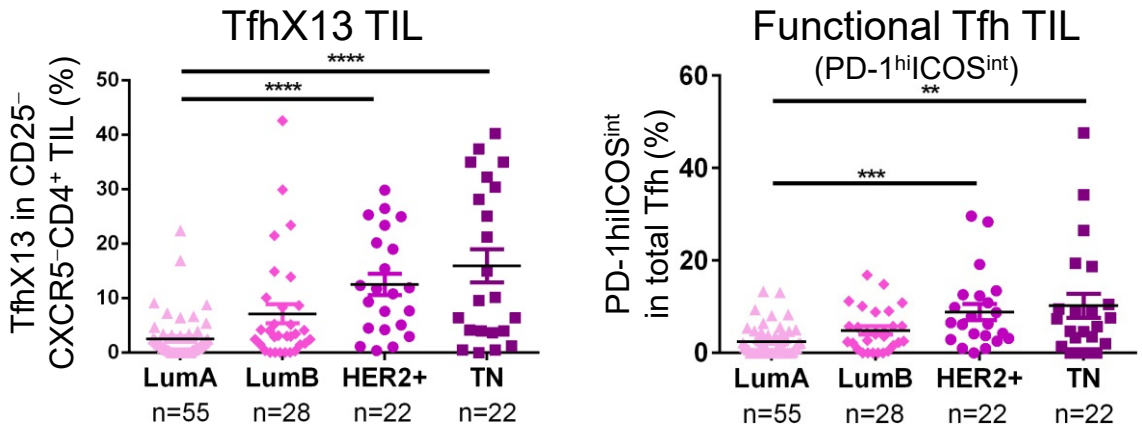

B Tonsillar CD4⁺ T cells

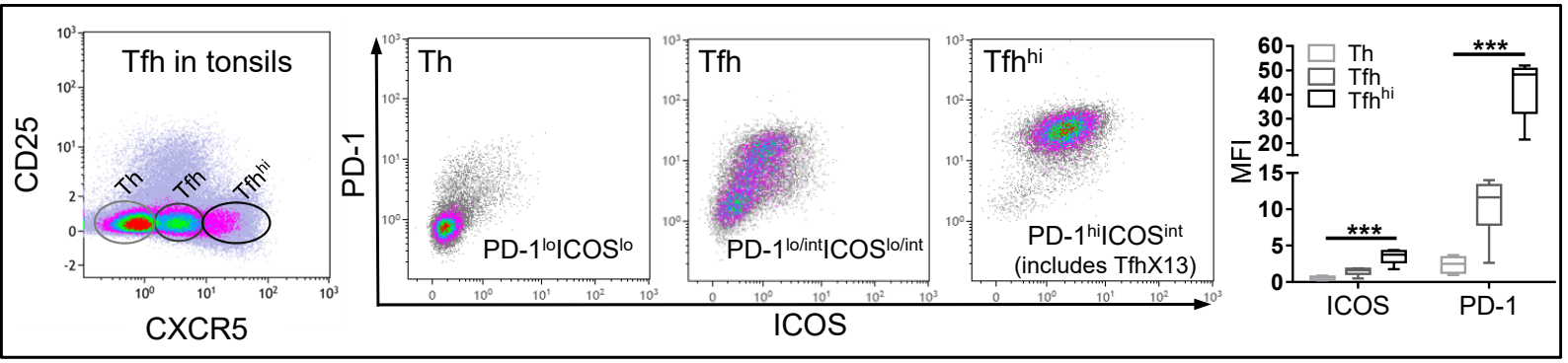

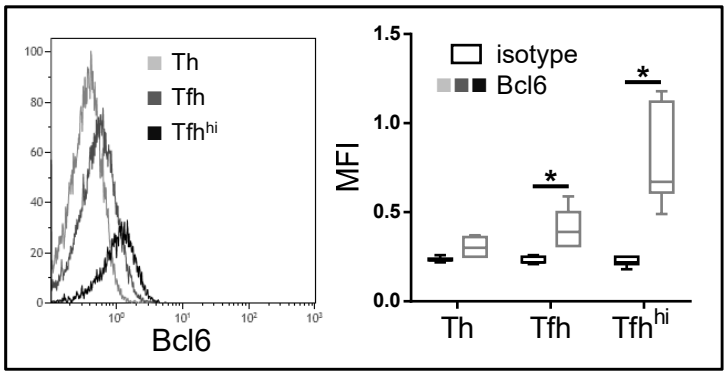

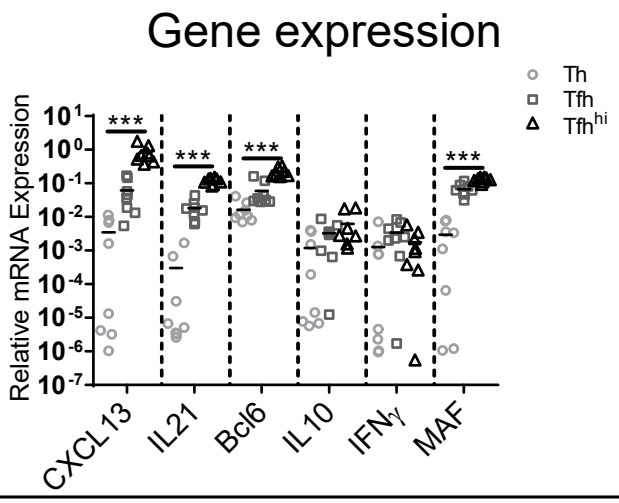

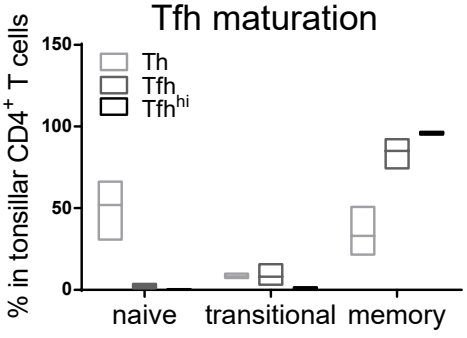

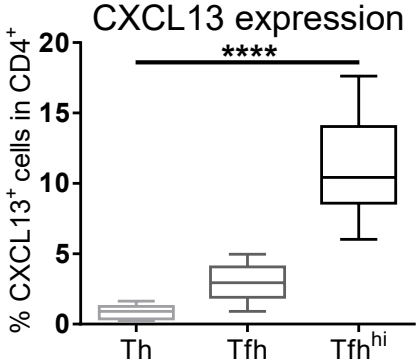

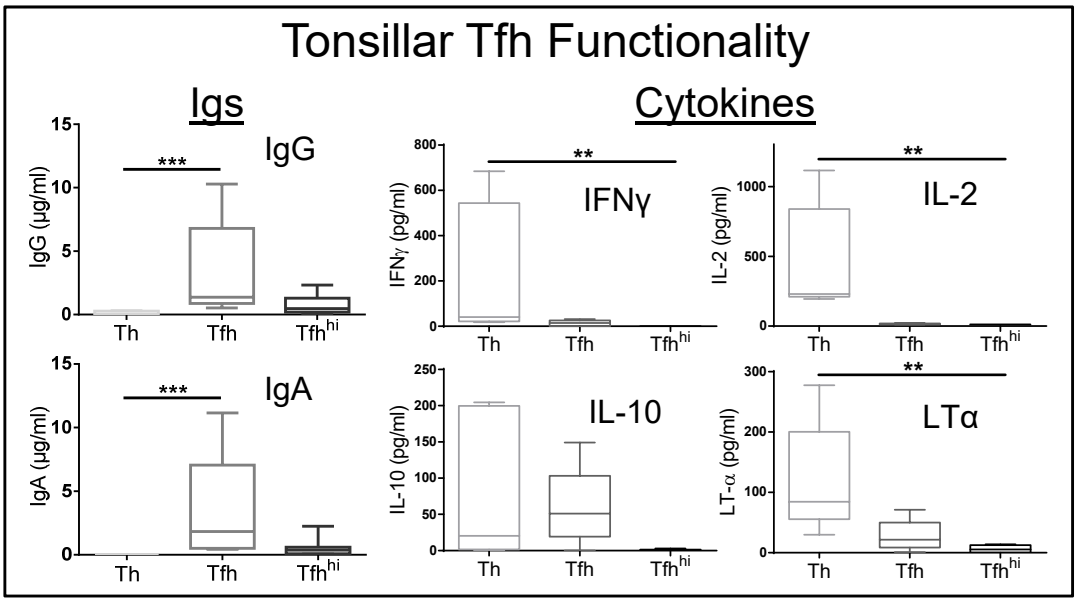

C CD4+ Tfh TIL in BC

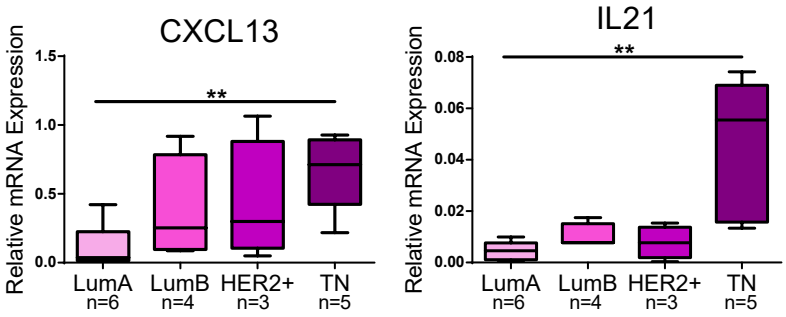

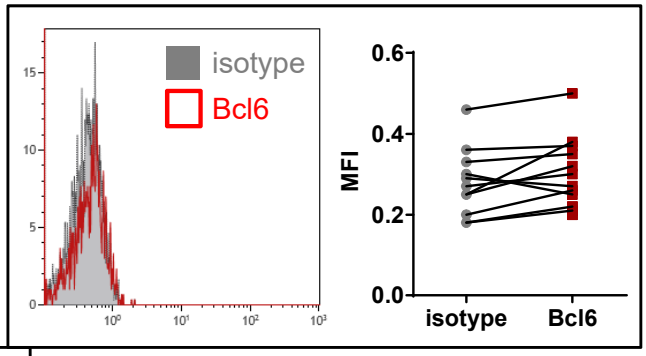

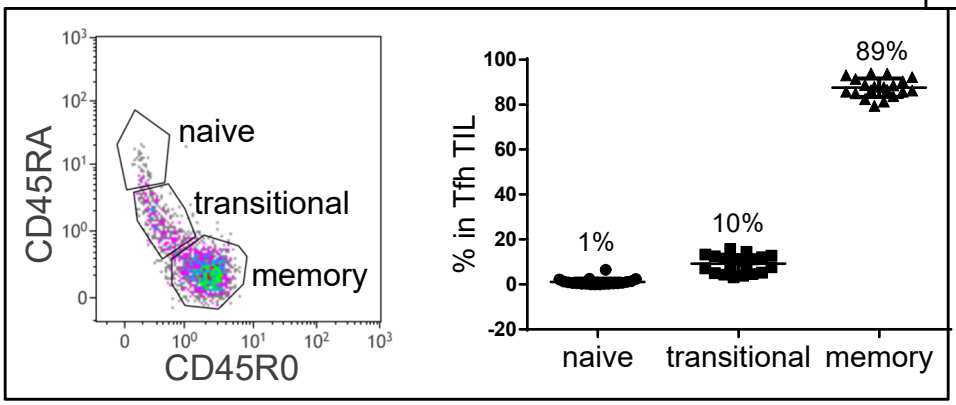

D Immunofluorescent confocal microscopy

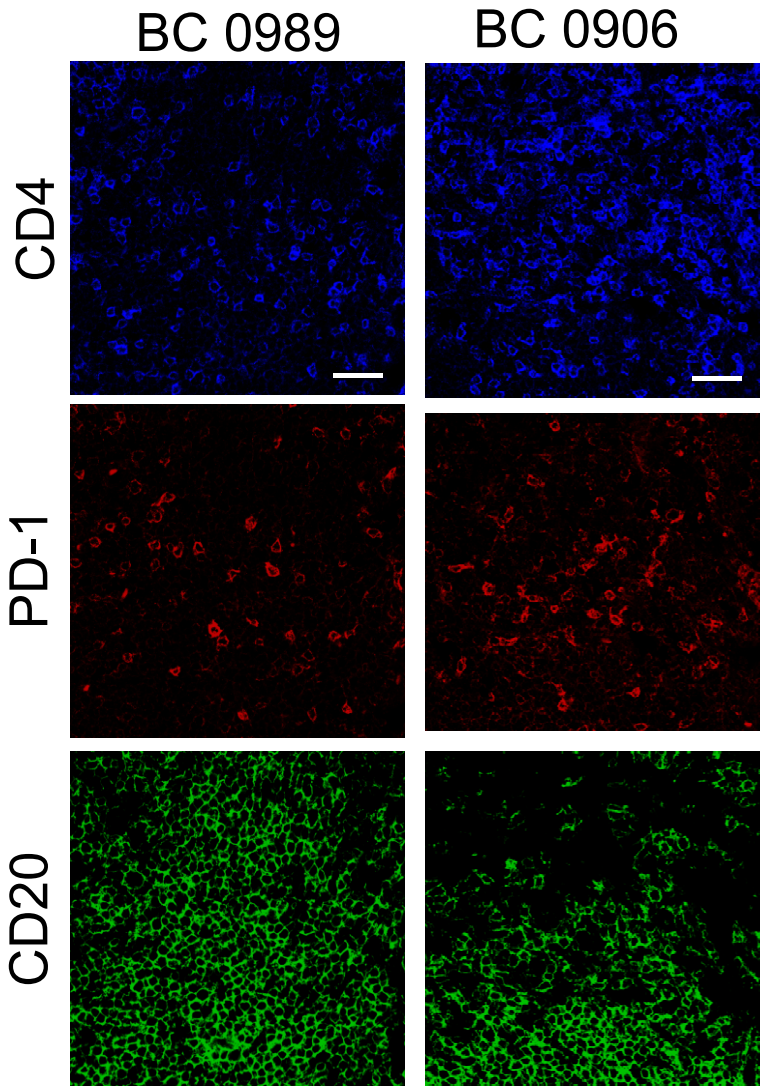

Individual stains for Figure 2C

E Control of CD4⁺ TIL activation (3d)

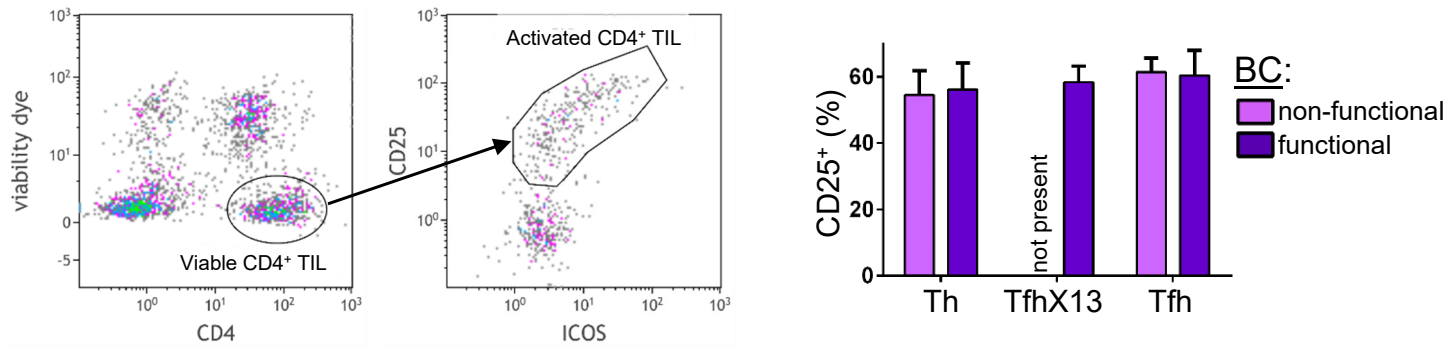

Supplemental Figure 2

A. *Left graph*: TfhX13 TIL frequencies in $CD25^{-}CXCR5^{-}$ TIL. *Right graph*: functional Tfh TIL ($PD\text{-}1^{hi}ICOS^{int}$; functionality is demonstrated in the next section) in total Tfh TIL from the BC subtypes [N=127; LumA (N=55), LumB (N=28), HER2+ (N=22), TN (N=22)].

B. *Top left graph*: flow cytometric analysis of CXCR5 expression on tonsillar $CD4^{+}CD25^{-}$ T cells: Th cells = $CXCR5^{-}$, Tfh cells = $CXCR5^{int}$ and Tfh^{hi} cells = $CXCR5^{hi}$. *Top middle panels:* ICOS and PD-1 expression on the Th, Tfh and Tfh^{hi} subpopulations is shown. *Top right panel*: mean fluorescent intensities for ICOS and PD-1 on the Th, Tfh and Tfh^{hi} subpopulations (N=7). *Middle left panels:* flow cytometric analysis of Bcl6 nuclear staining in the Th, Tfh and Tfh^{hi} subpopulations (N=7). *Middle right graphs*: gene expression analysis in the Th, Tfh and Tfh^{hi} subpopulations (N=7). *Lower left graphs*: flow cytometric analysis of surface CD45RA/RO (naïve/memory distribution) and intracytoplasmic CXCL13 in the Th, Tfh and Tfh^{hi} subpopulations (N=7). *Lower right graphs*: the Th, Tfh and Tfh^{hi} tonsillar subpopulations were sorted and activated in the Tfh functional assay. Igs and cytokines in the culture supernatant were quantified a day 7 (N=7).

C. *Upper left graphs*: gene expression analysis of CXCL13 and IL-21 in sorted Tfh TIL divided by BC subtype. *Upper right panels*: flow cytometric analysis of Bcl6 nuclear staining in Tfh TIL (N=14). *Lower left panels*: flow cytometric analysis of surface CD45RA/RO expression for Tfh TIL naïve to memory cell distribution (N=20).

D. Individual IF stains for CD4 (blue), PD-1 (red) and CD20 (green) captured by confocal microscopy. White scale bars = 35μm.

E. *Left panels*: The gating strategy shown was used to analyze ICOS and CD25 expression on viable $CD4^{+}$ TIL at day 3 of the Tfh functional assay. *Right panel*: activated cell frequencies (% of $CD25^{+}$ cells) within the Th, TfhX13 or Tfh TIL subpopulations after activation in the Tfh functional assay are shown. The Th, TfhX13 or Tfh TIL subpopulations are divided on the basis of functional or non-functional Tfh TIL in corresponding BC tumor directly *ex vivo* (detailed in the legend for Figure 2E).

Supplemental Figure 3
Noël, *et al.*

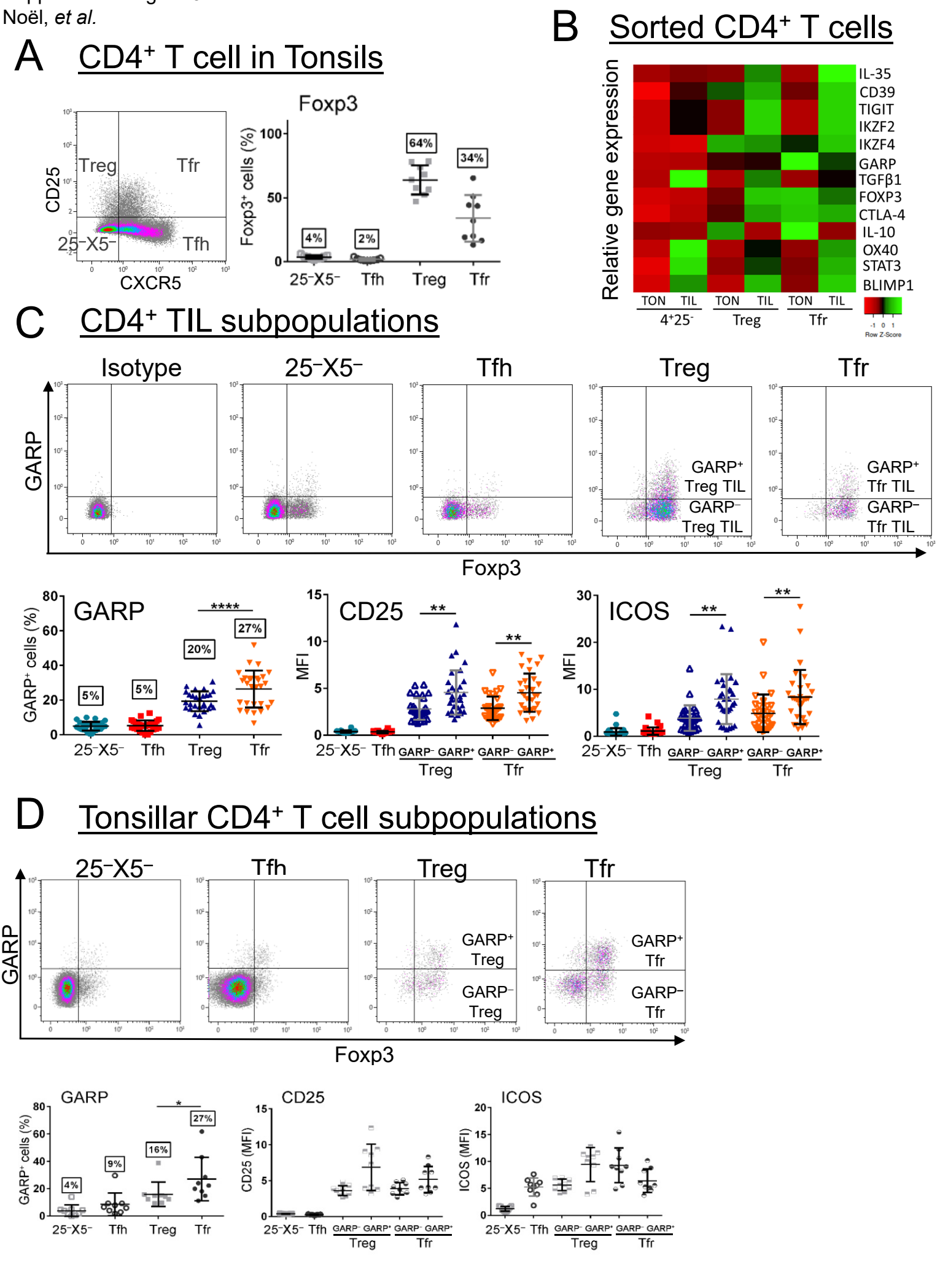

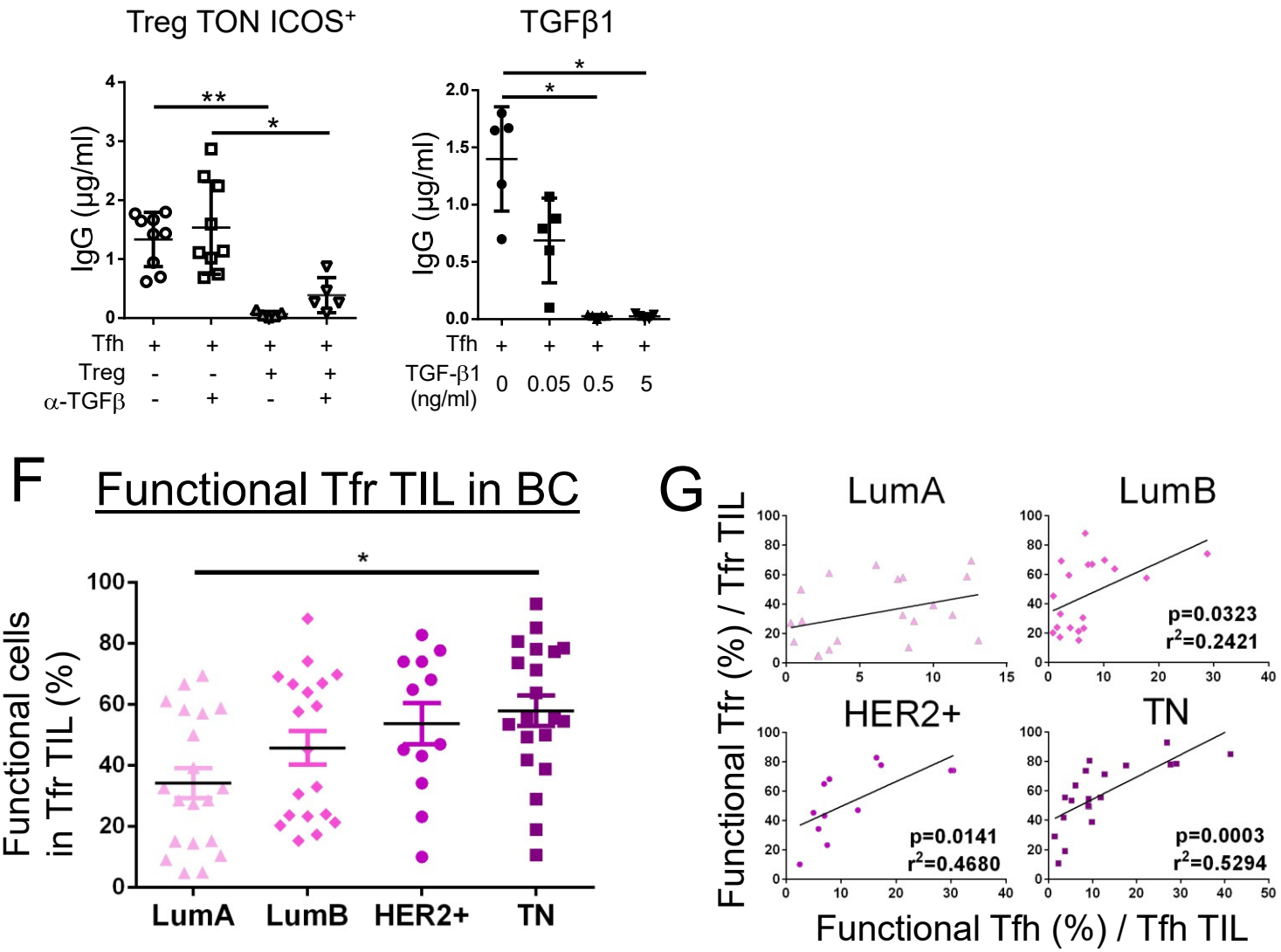

Supplemental Figure 3

A. Using flow cytometric analysis, tonsillar $CD4^+CD25^+$ T cells are divided into two subpopulations: Treg ($CXCR5^-$) and Tfr ($CXCR5^+$). Foxp3 protein expression by tonsillar $CD4^+$ T cells was analyzed by intranuclear staining and flow cytometry (left panel, N=8).

B. Differential expression of key regulatory genes in sorted $CD4^+CD25^-$ Th, Treg and Tfr cells from tonsils (TON) or BC (TIL)

C and D. Example of gating strategies for analyzing Foxp3 and GARP expression on (C) $CD4^+$ TIL or (D) tonsillar $CD4^+$ T cell subpopulations (upper panels). The frequency of $GARP^+$ cells in (C) $CD4^+$ TIL or (D) tonsillar $CD4^+$ T cell subpopulations (lower left panel). Treg and Tfr cells from (C) BC or (D) tonsils are divided in two groups based on GARP expression and the mean fluorescence intensity of CD25 (lower middle panel) and ICOS (lower right panel).

E. Sorted tonsillar Treg were activated in presence of tonsillar Tfh cells with or without a functional anti-TGFβ antibody using our Tfh functional assay (left panel). TGF-β1 (different concentrations) were added (or not) in the Tfh functional assay using tonsillar Tfh cells (right panel).

F. Functional ($ICOS^{hi}PD\text{-}1^{int}$) Tfr TIL frequencies in total Tfr TIL in the individual BC subtypes [N=71; LumA (20), LumB (19), HER2+ (12), TN (20)].

G. The correlation between functional Tfh and Tfr TIL frequencies in the individual BC subtypes [N=71; LumA (20), LumB (19), HER2+ (12), TN (20)].

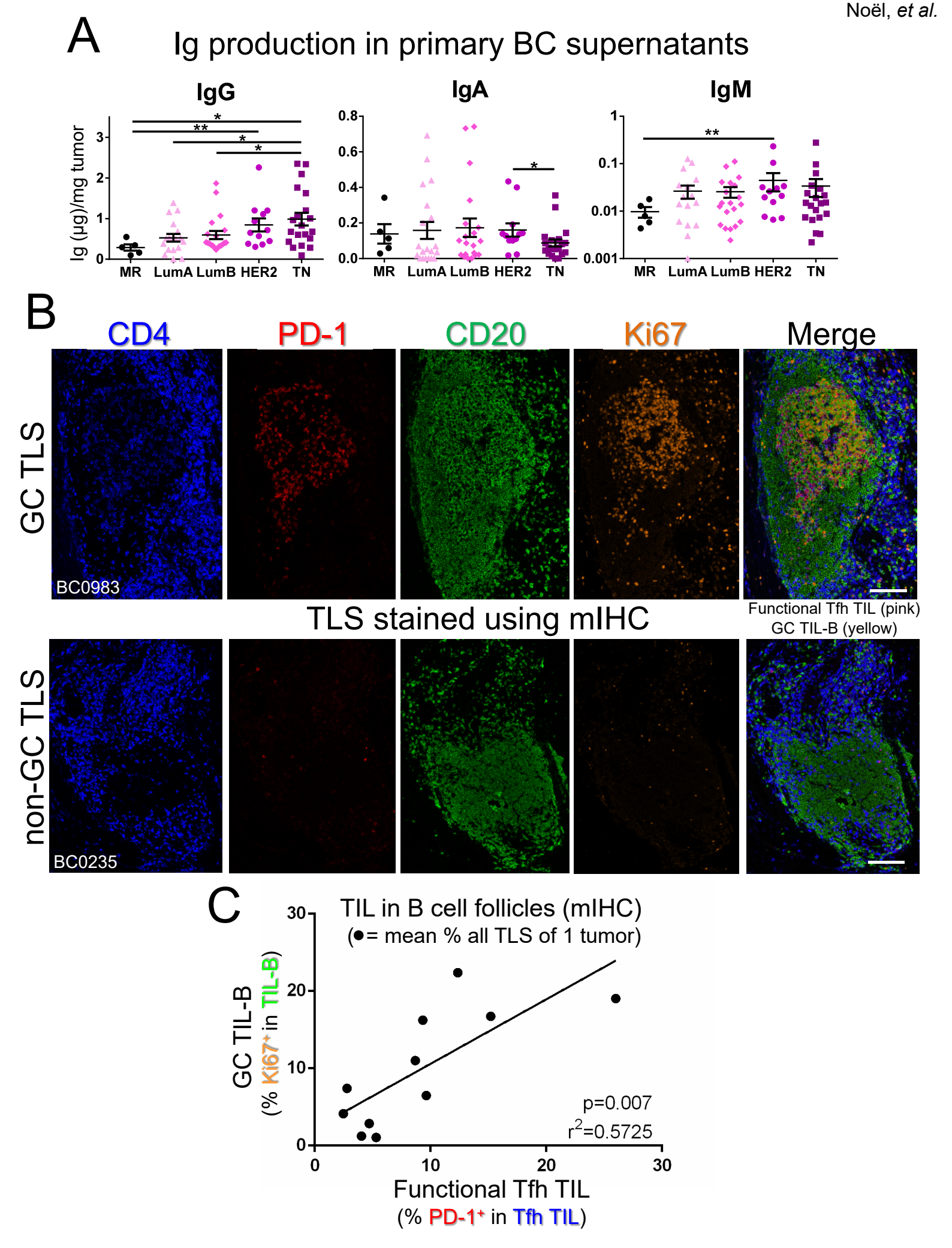
A
Ig production in primary BC supernatants
IgG
IgA
IgM
Ig (µg)/mg tumor
MR
LumA
LumB
HER2
TN
B
CD4
PD-1
CD20
Ki67
Merge
GC TLS
BC0983
TLS stained using mIHC
Functional Tfh TIL (pink)
GC TIL-B (yellow)
non-GC TLS
BC0235
C
TIL in B cell follicles (mIHC)
(●= mean % all TLS of 1 tumor)
GC TIL-B
(% Ki67+ in TIL-B)
p=0.007
r2=0.5725
Functional Tfh TIL
(% PD-1+ in Tfh TIL)

D Individual antibody staining for Figure 4E (mIHC)

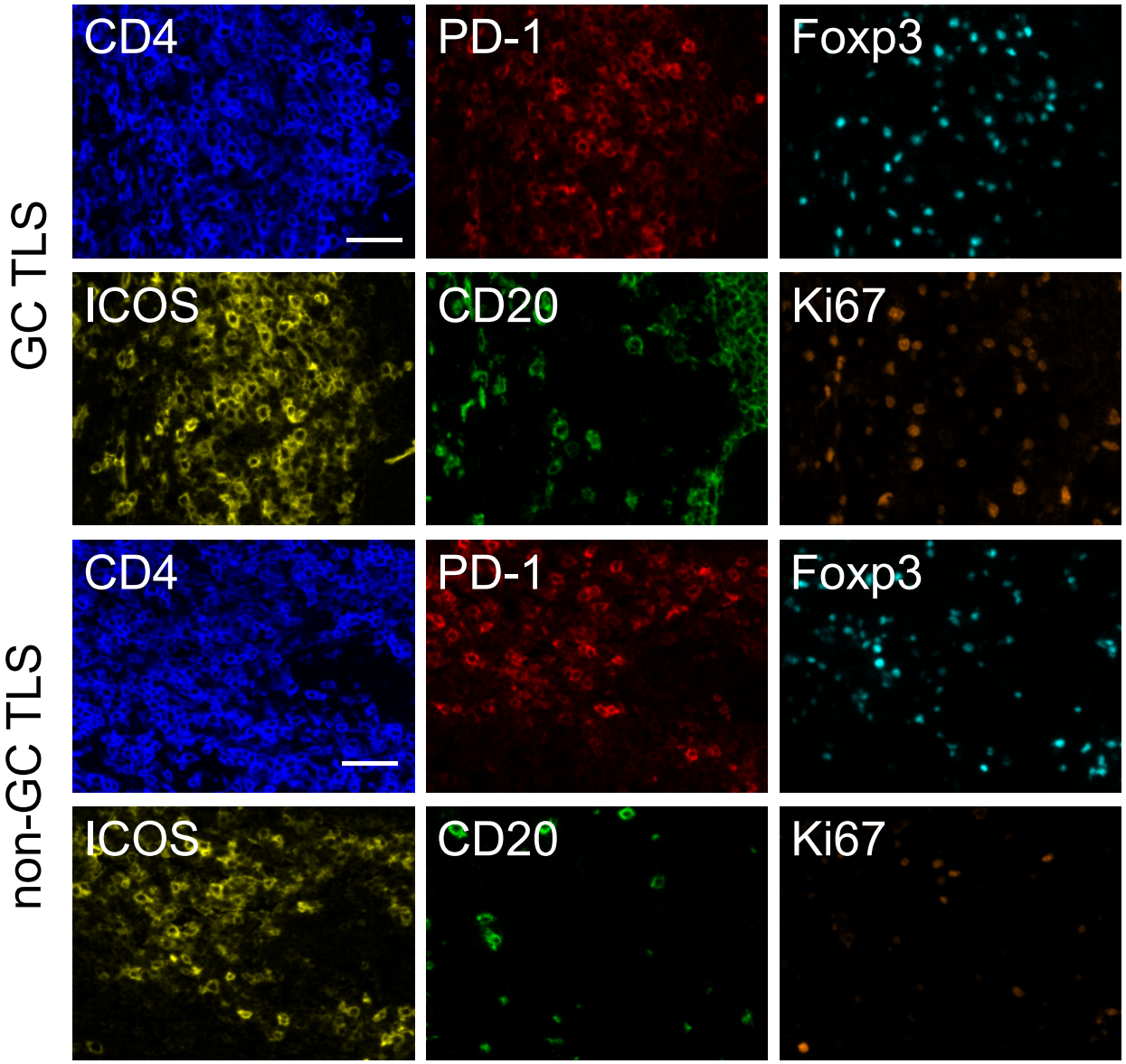

E

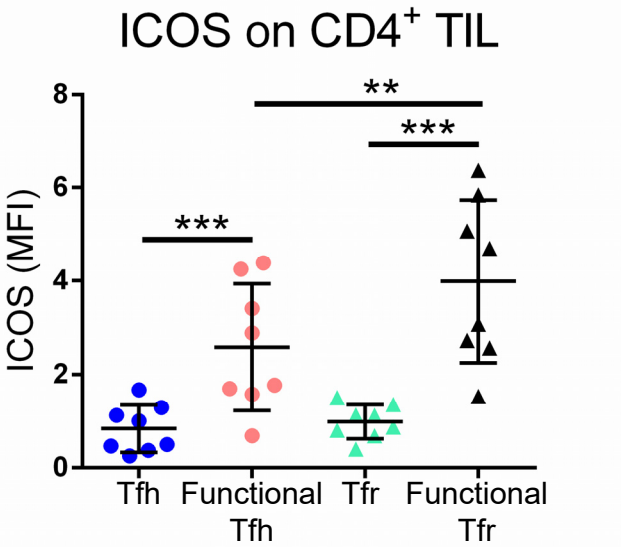

F

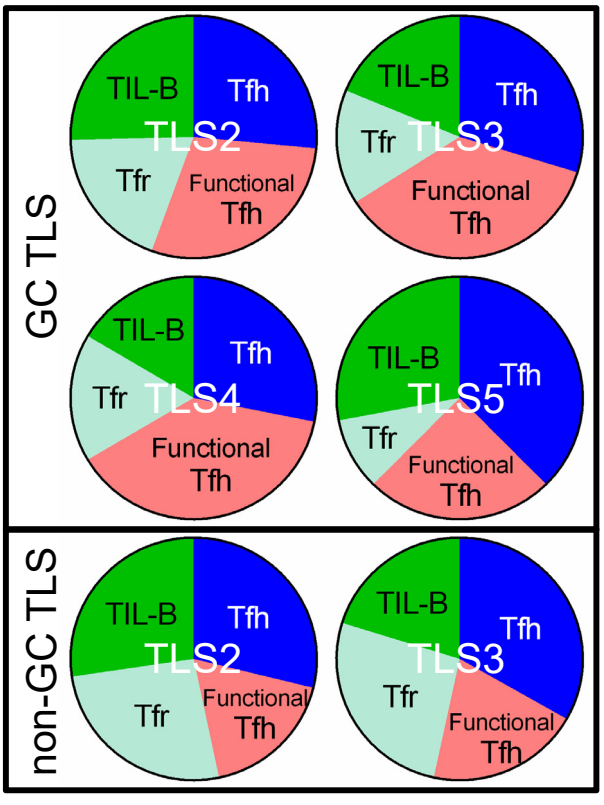

Supplemental Figure 4

A. Ig production [Ig (μg) / tumor (mg)] quantified in fresh tissue supernatants from mammary reductions (n=5; control) and the BC subtypes: LumA (N=20); LumB (N=19); HER2+ (N=12); and TN (N=20).

B. Images of multiplex IHC (mIHC) stained for CD4 (blue), CD20 (green), PD-1 (red) and Ki-67 (orange) showing tissue from two representative TN BC; *upper panels*: GC^+ TLS and *lower panels*: GC^- TLS; white scale bars = 200μm.

C. Correlation between the frequency of functional Tfh ($PD\text{-}1^+$) in total Tfh TIL and proliferating cells ($Ki\text{-}67^+$) in total TIL-B from TLS (mIHC-stained as in **B**) from HER2+ and TN BC; each point represents the mean score for all TLS in an individual tumor (N=11).

D. Individual mIHC-stained images for CD4 (blue), PD-1 (red), Foxp3 (cyan), ICOS (yellow), CD20 (green) and Ki-67 (orange); merged image is shown in Figure 4E; white scale bars = 50μm.

E. ICOS expression was quantified for Tfh ($PD\text{-}1^-$), functional Tfh ($PD\text{-}1^+$), Tfr ($ICOS^-$) and functional Tfr ($ICOS^+$) in TLS (N=8) using the mIHC panel in **D**.

F. The number of functional Tfr TIL ($CD4^+Foxp3^+ICOS^+$) touching Tfh TIL ($CD4^+PD\text{-}1^-$) or functional Tfh TIL ($CD4^+PD\text{-}1^+$) or Tfr TIL ($CD4^+Foxp3^+ICOS^-$) or TIL-B ($CD20^+$) in the T cell zone is shown for six additional TLS (2 other TLS are shown in Figure 4E).

A

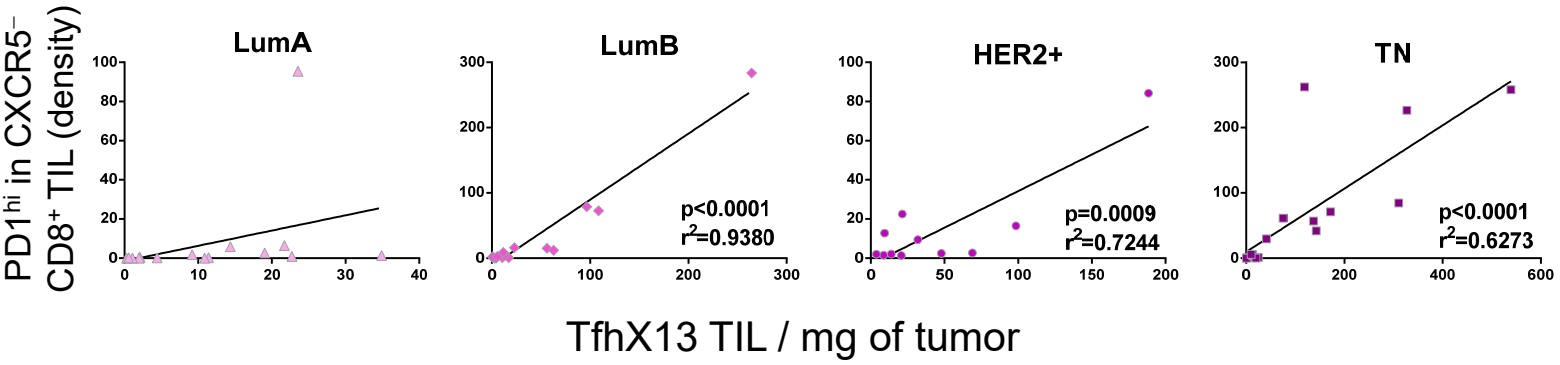

B Individual mIHC stains for Figure 5E

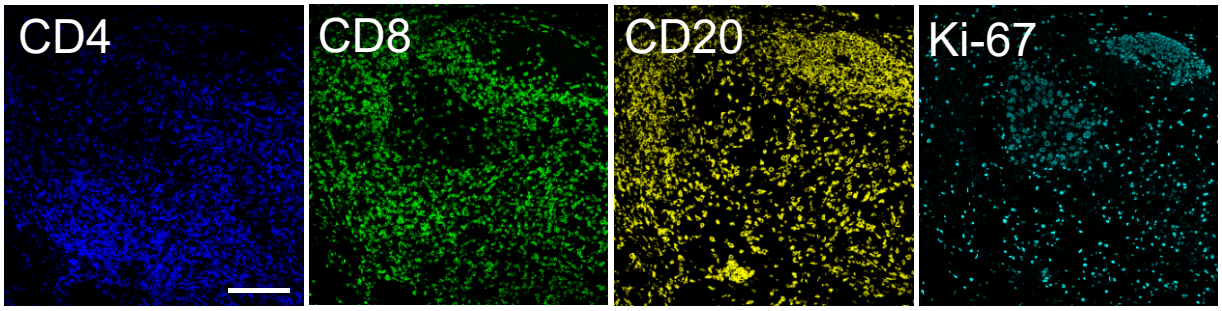

Zoom GC

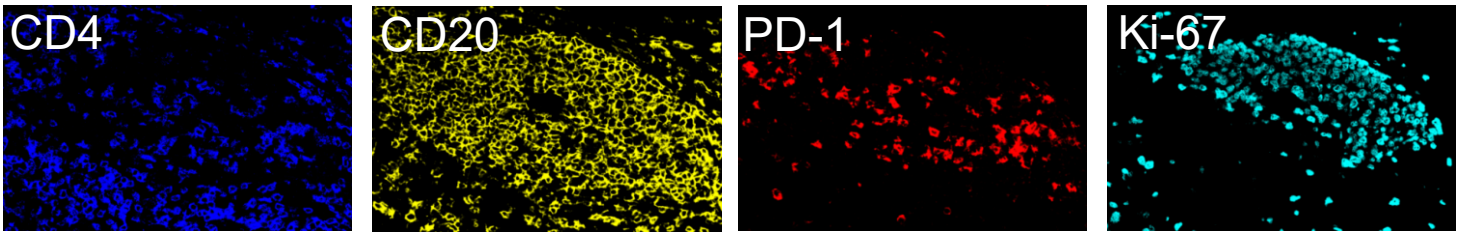

Zoom 1

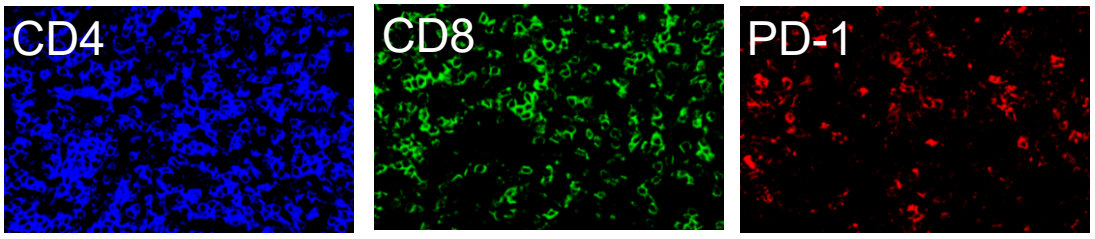

Zoom 2

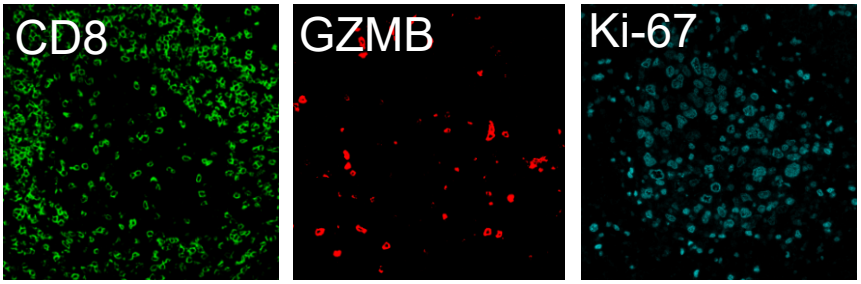

for Figure 5G

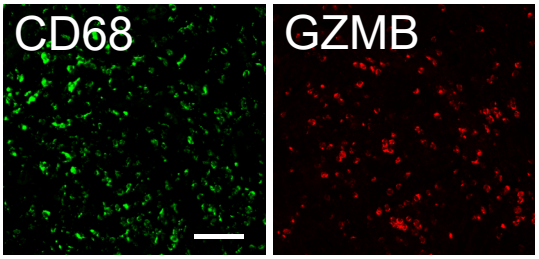

C TLS lacking a GC (mIHC)

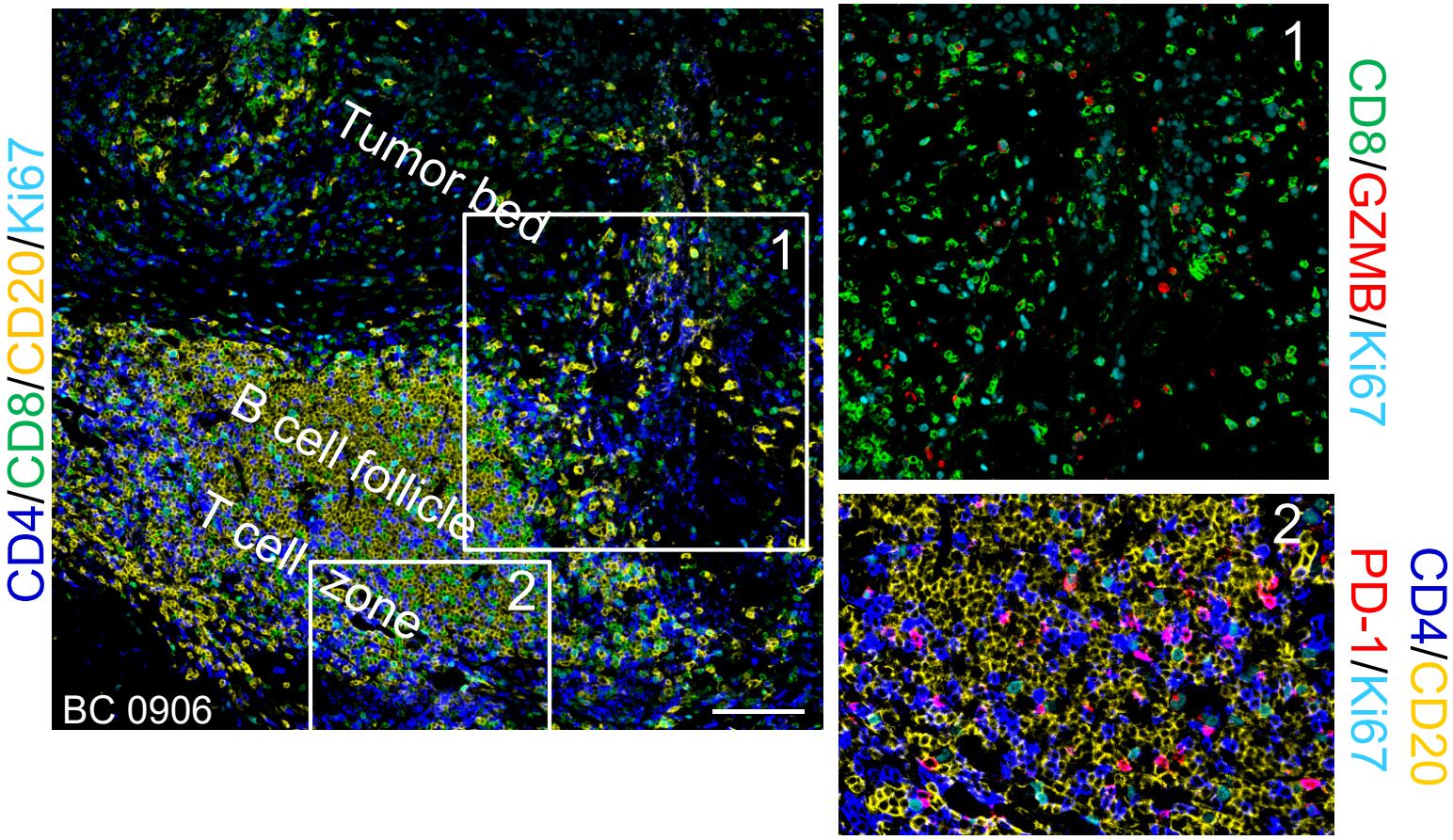

D Merge and Individual mIHC stains for Figure 5F

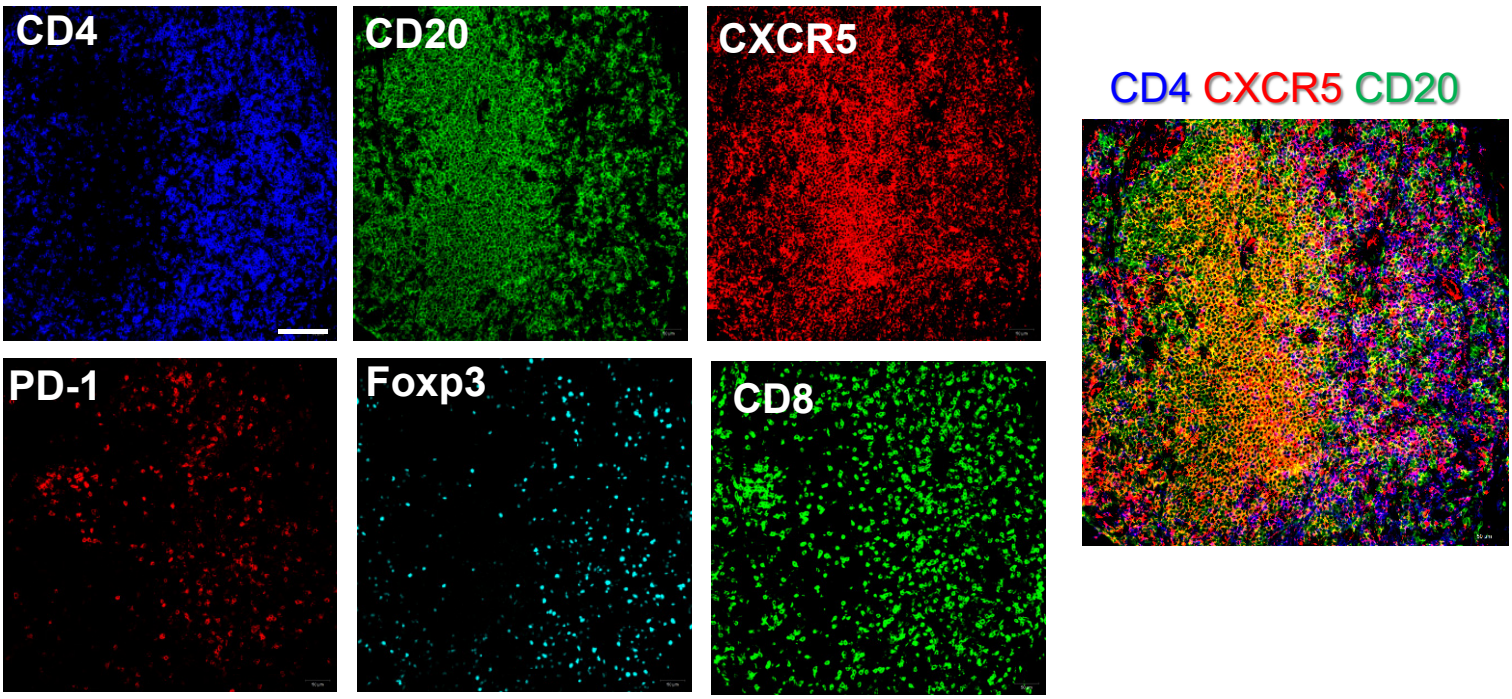

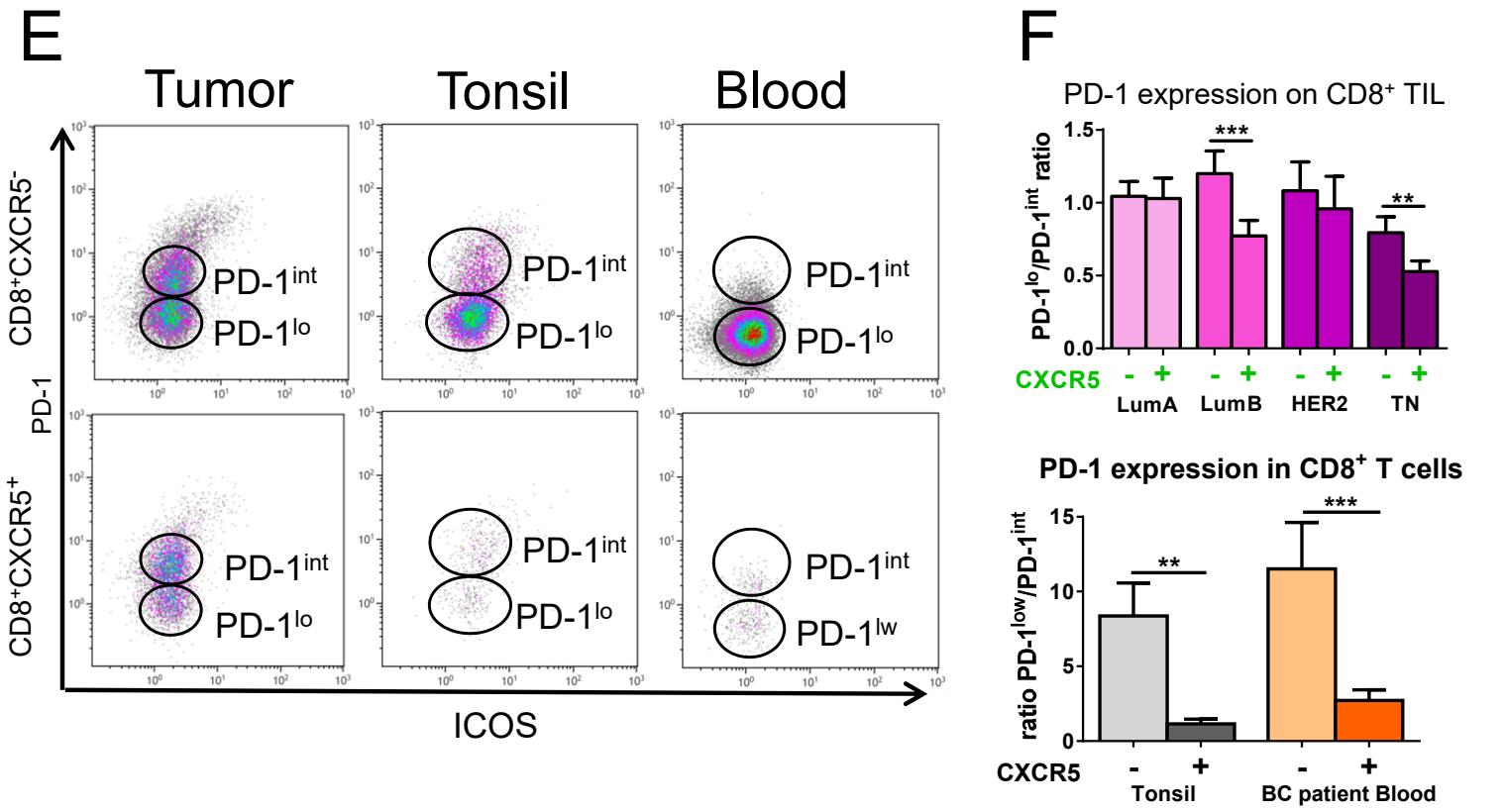

TN Breast Cancer

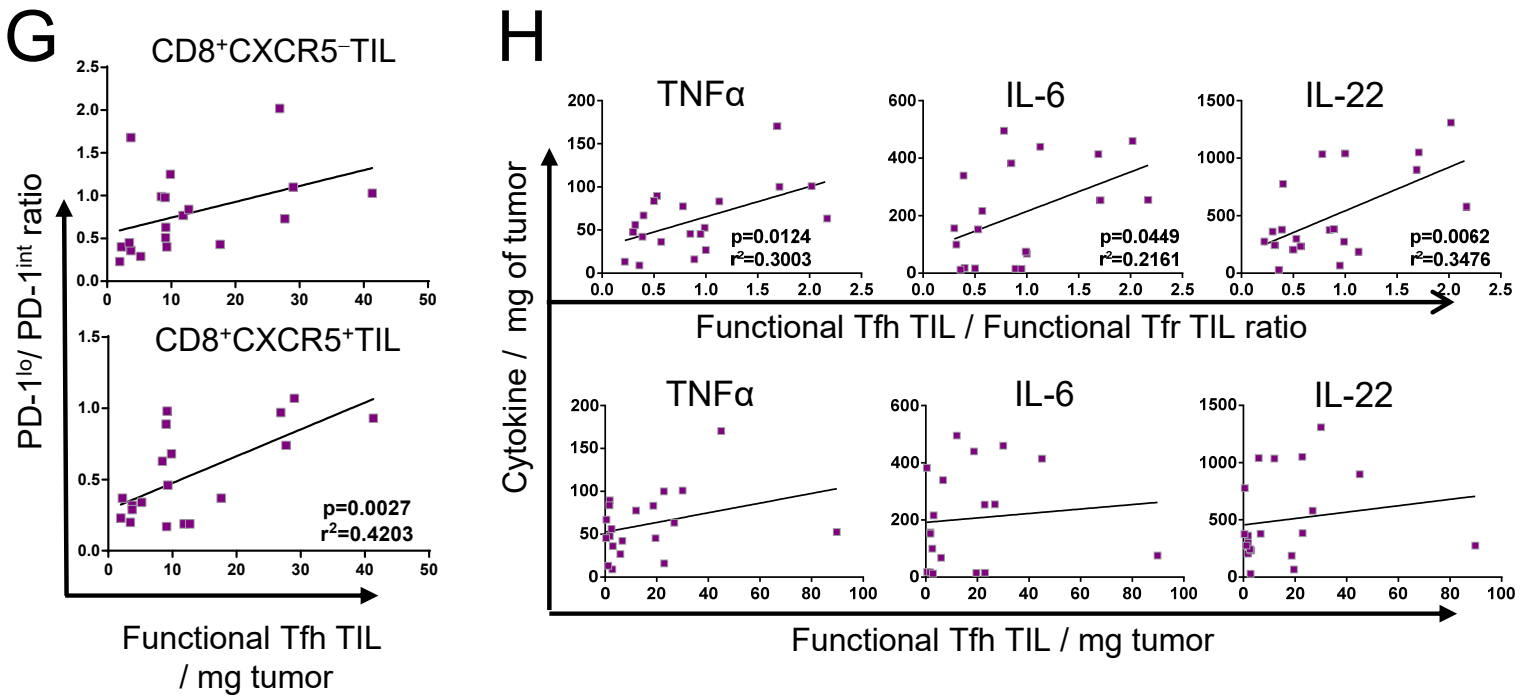

Supplemental Figure 5

A. Correlation between the density of TfhX13 TIL and activated $CD8^+CXCR5^+PD\text{-}1^{hi}ICOS^{int}$ TIL in the different BC subpopulations [N=71; LumA (N=20), LumB (N=19), HER2+ (N=12), TN (N=20)].

B. Individual mIHC stains for the merged images shown in Figure 5E of a representative tumor (BC 1068). *Upper 3 panels including global, zoom GC and zoom 1*: CD4 (blue), CD8 (green), CD20 (yellow), PD-1 (red) and Ki-67 (cyan), white scale bar = 150μm. *Zoom 2*: CD8 (green), granzyme B (red) and Ki-67 (cyan). Individual mIHC stains for the merged images shown in Figure 5G of a representative tumor (BC 0906). *Lower right panels*: CD68 (green) and GZMB (red), white scale bar = 80μm.

C. *Left panel*: mIHC stained FFPE tumor section showing a TLS (TN BC 0906); CD4 (blue), CD8 (green), CD20 (yellow) and Ki67 (cyan), white scale bars = 150μm. *Zoom 1, upper right*: CD8 (green), GZMB (red) and Ki67 (cyan); granzyme B expression detected in $CD8^+$ TIL (green membrane and red cytoplasm) and $CD4^-CD8^-CD20^-$ cells (red inter-membrane staining) both in close contact with tumor cells (cyan nucleus). *Zoom 2, lower right*: CD4 (blue), CD20 (yellow), PD-1 (red) and Ki67 (cyan) showing $PD\text{-}1^+CD4^+$ TIL (surrogate for functional Tfh TIL, pink) in a B cell follicle without a GC.

D. Individual mIHC stains. *Left panels*: CD4 (blue), CD20 (green), CXCR5 (red), PD-1 (red), Foxp3 (cyan) and CD8 (green) for the merged images shown in Figure 5F. *Right panel*: merged image for CD4, CD20 and CXCR5 showing $CD4^+CXCR5^+$ (purple) and $CD20^+CXCR5^+$ (yellow) TIL. White scale bars = 80μm.

E. The gating strategies used to divide $CD8^+CXCR5^-$ and $CD8^+CXCR5^+$ T cells in $PD\text{-}1^{lo}$ and $PD\text{-}1^{int}$ subpopulations from tumor, tonsils and BC patient blood.

F. The ratio between $PD\text{-}1^{lo}$ cells and $PD\text{-}1^{int}$ cells in $CD8^+CXCR5^-$ and $CD8^+CXCR5^+$ T cells is shown. *Upper graph*: TIL in individual BC subtypes and *lower graph*: T cells in human tonsils and BC patient blood.

G. The density of functional Tfh TIL (number/mg of tumor) is correlated with the $PD\text{-}1^{lo}$ to and $PD\text{-}1^{int}$ ratios in *upper graph*: $CD8^+CXCR5^-$ TIL or *lower graph*: $CD8^+CXCR5^+$ TIL in TN BC (N=18). The densities and ratios were based on flow cytometric data.

H. Correlations between ratios. *Upper graphs*: functional Tfh to functional Tfr TIL and *lower graphs:* functional Tfh TIL to the density (number of TIL/mg of tumor) correlated with TNFα, IL-6 and IL-22 (μg of cytokine/mg of tumor) quantified in the corresponding primary tumor supernatants from TN BC (n=20). The density and ratio were determined by flow cytometry.

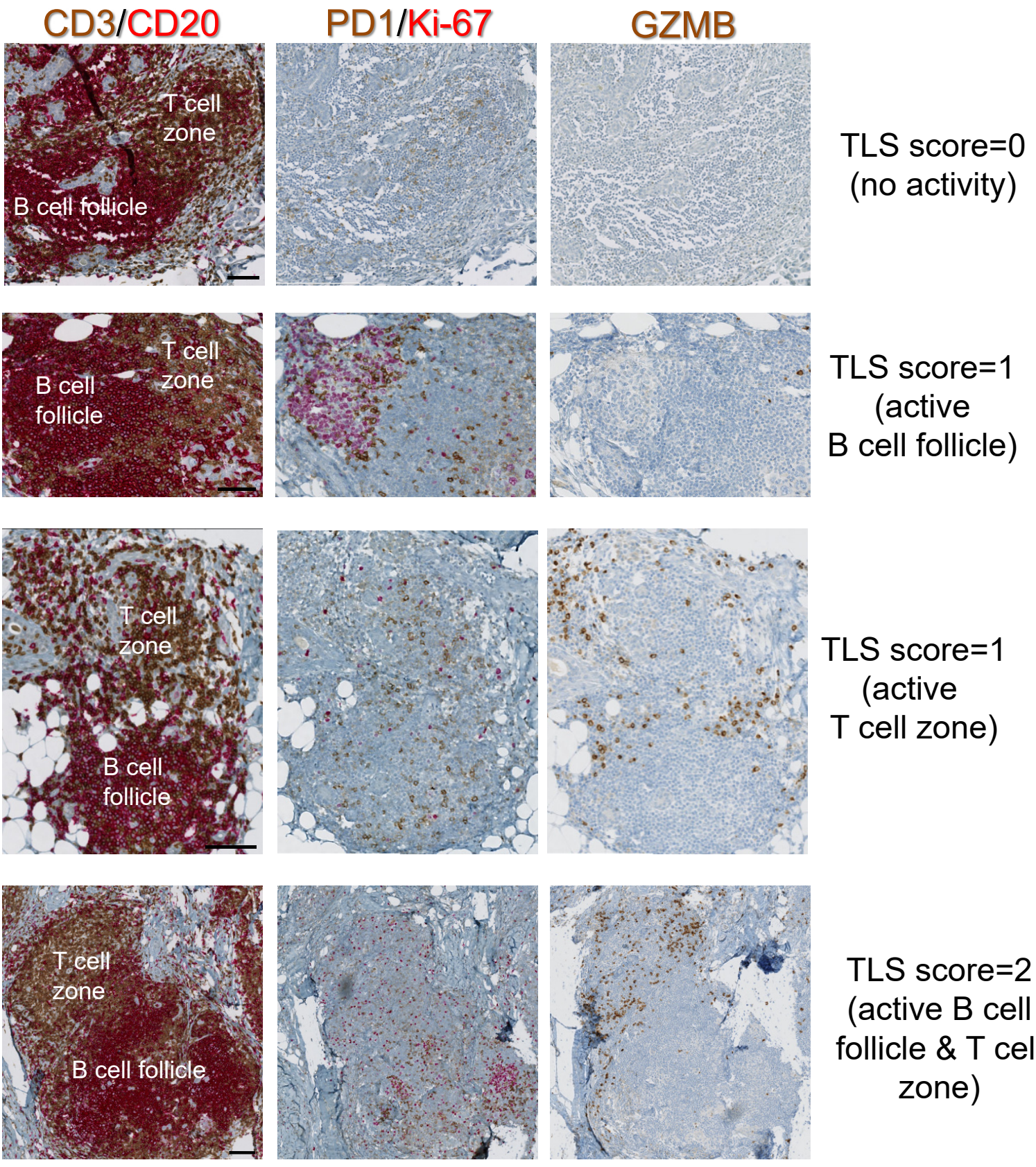
CD3/CD20
PD1/Ki-67
GZMB
T cell zone
B cell follicle
TLS score=0 (no activity)
T cell zone
B cell follicle
TLS score=1 (active B cell follicle)
T cell zone
B cell follicle
TLS score=1 (active T cell zone)
T cell zone
B cell follicle
TLS score=2 (active B cell follicle & T cell zone)

Supplemental Figure 6

Examples of TLS stains using three consecutive FFPE tumor sections from selected TN or HER2+ human BC that were scored for TLS: dual IHC for CD3 (brown) and CD20 (red) (left panels); dual IHC for PD-1 (brown) and Ki-67 (red) (middle panels); single IHC for granzyme B (right panels). Upper panels: TLS score=0, no activity in either TLS zone. Upper middle panels: TLS score=1, the presence of germinal center (GC) in the B cell follicle is detected, no activity is observed in the T cell zone. Lower middle panels: TLS score=1, no GC in the B cell follicle, PD-1 and GZMB expression are detected in the T cell zone. Lower panels: TLS score=2, a GC is present in the B cell follicle and PD-1 and GZMB expression is detected in the T cell zone. Black scale bars: 100μm.

Supplemental Material & Methods

Noël *et al*.

SUPPLEMENTARY MATERIALS AND METHODS

Tumor infiltrated, tonsil and spleen lymphocytes

Dissected tumor fragments from fresh surgical specimens were processed as previously described[35]. Briefly, dissected breast tissues fragments from fresh surgical specimens were directly transferred into 3ml of X-VIVO 20 (Lonza). Tissue was manually minced before two rapid rounds of mechanical dissociation with the GentleMACS™ Dissociator (Program A.01; Myltenyi Biotec). The resulting cell suspension was filtered following each dissociator run using a 40µm cell strainer (BD Falcon), washed with X-VIVO 20, centrifuged 15min at 600g, and resuspended in X-VIVO 20 before flow cytometric analysis. The tumor supernatant was the initial 3ml of X-VIVO 20 recovered after the first round of dissociation, which was subsequently clarified by centrifugation for 15 min at 13000g.

Tonsil and spleen fragments from fresh surgical specimens were directly transferred into 3ml of X-VIVO 20 and then manually and mechanically dissociated, following by 40µm cell strainer filtration. Tonsil and spleen lymphocytes, like PBMC from blood, were then purified by density gradient centrifugation over Lymphoprep™ and washed three times before FACS staining.

Flow cytometry

Cell suspensions were incubated according to the manufacturer's suggested dilutions of fluorescently labeled primary monoclonal antibodies (listed in Table S9) for 20 minutes at 4°C in 100ul of facs buffer (PBS with 2% of FBS, 1mM of EDTA and 0.1% of sodium azide) followed by washing with PBS. After red blood cells lysis (VersaLyse, Beckman Coulter), cells were immediately acquired on a GALLIOS 10/3 cytometer (Beckman Coulter) and results analyzed with Kaluza Flow Cytometry Analysis v1.5 software. 123 Count ebeads (eBioscience, ThermoFisher) was added before cytometry acquisition for TIL quantification in order to calculate TIL density. Intracellular staining was used for Foxp3 and CXCL13 using Foxp3/Transcription Factor Staining Buffer Set (eBioscience, ThermoFisher) without using Golgi-stop reagents. Anti-GARP antibody (MHG-6) is a kindly gift of DeDuve Institut[69].

Cell sorting was performed on tumor or tonsil cell suspension using a Moflo ASTRIOS EQ 12/4 sorter (Beckman Coulter). Purity of sorted cells was control in the GALLIOS 10/3 cytometer and consider acceptable when ≥ 95%.

Cytokine and Ig measurement in supernatant

Ig concentrations in tumor supernatant and in culture supernatant of the Tfh functional assay are measured using the BD cytometric bead array (CBA) Immunoglobulin master buffer kit (558683). Cytokine concentration in culture supernatant of the Tfh functional assay is measured using the BD CBA Soluble Protein master buffer kit (558264, BD Bioscience). Cytokine concentration in tumor supernatant is measured using the Human Th cytokine Panel (13-plex) LEGENDplexTM (BioLegend). All kits are used according to the manufacturers' instructions.

Immunohistochemistry staining and Immunofluorescence microscopy

Formalin-fixed paraffin embedded (FFPE) sections (4 µm) from available tumor tissues were deparaffinized and demasked prior to antibody labeling. Antibodies are listed in the table S10. cIHC antibody staining on full-face sections was performed using the iVIEW DAB Detection Kit and a BenchMark XT IHC/ISH automated slide stainer (Discovery XT, Tucson, USA). Slides were lectured by two trained pathologists. cIHC images were acquired at Lens 20x with a Nanozoomer 2.0-RS Digital slide scanner (Hamamatsu) and analyzed using NDP.view2 software. TLS and TIL aggregates were scored using a dual CD3/CD20 cIHC on FFPE tumor section from human BC. TLS represent an organized TIL structure with distinguished T cell zone and B cell follicle while TIL aggregates is just a unorganized cluster of TIL. For quantification of TLS activities, a dual PD-1/Ki67 cIHC and a single GZMB cIHC was used on FFPE consecutive sections following this used for CD3/CD20 cIHC.

FFPE blocs were also analyzed by immunofluorescence. Mounted sections were deparaffinized with xylene, pretreated with citrate 10mM, pH 6.0 at 95°C for 30min, blocked with 1% BSA for 30min prior to incubation with a mixture of three primary antibodies (listed in the table S11) in a moist chamber at 4°C overnight. After wash, a mixture of three secondary antibodies (listed in the table S10) was added for two hours at room temperature followed by mounting in a Prolong Gold Antifade Reagent with DAPI (Life Technologies). Confocal imaging was realized on a Zeiss LSM-710 confocal microscope using a Zeiss x20/0,8 PlanApochromat objective with specific excitation using a 488nm Argon ion laser, a 543nm laser diode and a 633nm Helium/Neon laser. Fluorescence detection was done sequentially through a 1 Airy Unit pinhole and PMT detectors. Images were acquired using Zeiss ZenBlack software (Zeiss, Oberkochen, Germany) at 20X Magnification and analyzed using ZEN software. Colocalization analyses were done using Fiji software[71] and the JACOP plugin[72]. Briefly, background signal of images was reduced using a 1 pixel radius median filter and Pearson's and Mander's coefficients were analyzed using an automatic threshold. The cytofluorograms were obtained using the Coloc2 Plugin.

Fluorescent multiplex IHC (mIHC)

Multiplex IHC staining

Four mIHC panels were optimized to investigate the role of T_{FH} and T_{FR} cells in the immune response against Breast Cancer (BC) as detailed in Table S12. mIHC stainings were performed manually on formalin-fixed paraffin-embedded (FFPE) BC sections using Opal reagents (Akoya Biosciences, Menlo Park, CA). Briefly, the tissue sections were cut at a thickness of 4 µm and mounted on Superfrost Plus slides (Menzel-Glaser). The sections were deparaffinized with xylene, hydrated through an ethanol gradient and fixed in 10% neutral buffer formalin for 20 min. Heat-induced antigen retrieval or antibody stripping were achieved in Antigen Retrieval (AR) 6 or AR9 buffer (Akoya Biosciences) using a microwave (Panasonic with Inverter technology). The sections were brought to a boil at 100% power followed by 10% power for 15 min and then left to cool at least for 15 min. After a 10-minute block (Opal Antibody Diluent

/ Block, Akoya Biosciences), the sections were incubated with the primary antibody then with the horseradish peroxidase (HRP)-conjugated secondary polymer (anti-mouse/anti-rabbit, Akoya Biosciences) and finally with HRP-reactive Opal fluorophore for 10 min (Akoya Biosciences). The slides were washed between each step in 0.05% Tris-Buffered Saline–Tween 20 three times at 2 min each. After the final staining, the nuclei were counterstained with spectral DAPI (Akoya Biosciences) for 5 min and the slides were mounted in Vectashield Hard Set Medium (Vector Labs).

Multiplex IHC panel Optimization

Optimization and validation of mIHC panel were based on Akoya's recommendations. For each marker, the antigen retrieval condition, antibody titration, epitope sensitivity and antibody stripping were optimized in FFPE tonsil section. Opals were paired to primary antibodies taking account of Opal brightnesses, expression of the markers in the tissue of interest and their cellular localisation. Then Opal intensities were balanced in FFPE BC section and the crosstalks were evaluated using the unmixing quality report available in phenoptrReports package (Kent S Johnson (2020). In case of co-expressing markers, the TSA interferences were evaluated by comparing cell density and Opal mean expression between monoplex and mIHC slides. The staining order was defined based on epitope sensitivity and TSA interferences. Finally, mIHC panel were validated in FFPE BC section using the drop control method (3).

Multiplex IHC Acquisition and Quantification

The first mIHC panel targeting CD4, CD8, Foxp3, CD20, PD1 and CXCR5 was imaged using a Zeiss LSM confocal microscope equipped with PMT spectral 34 canaux QUASAR (Carl Zeiss) at 20X magnification. The other mIHC panels were imaged using the Vectra Polaris Automated Quantitative Pathology Imaging System (Akoya Biosciences). Whole-slides were scanned with all five standard epi-fluorescence filters (DAPI, FITC, Cy3, Texas Red and Cy5) at 20x magnification using appropriate exposure times. Then the regions of interest were selected for multispectral imaging at 20x magnification. To allow for unmixing of the multispectral images, a spectral library was generated from FFPE Tonsil sections. To build the library six slides were stained with a single Opal fluorophore without DAPI and one slide with DAPI only. The autofluorescence spectrum was generated from a FFPE BC section wherein no antibody, Opal reagent or DAPI was applied. The unmixing performance of the spectral library was assessed using the phenoptrReports' unmixing quality report. The multispectral images were unmixed using the spectral library and the tissue autofluorescence was removed in inForm Tissue Analysis Software (v2.4.8, Akoya Biosciences). The unmixed images of the mIHC panel targeting CD20, Ki67, CD4, PD1, ICOS and Foxp3 were analyzed using inForm software to segment tissue regions, segment cells, and phenotype the cells according to cell marker expression. The inForm datas were exported for analysis in RStudio IDE using the phenoptr and phenoptrReports packages. The cell density for each phenotype and Opal mean

expression of ICOS on different cell phenotype were generated using the merge cell seg files, the consolidate and summarize and the analyze consolidated data addins**.**

qRT-PCR

RNA was extracted from 1000 sorted TIL or tonsillar T cells using a SingleShot™ Cell Lysis Kit (1725080, BioRad) for nonadherent cells. Reverse transcription of the isolated RNA was done with the High-Capacity RNA-to-cDNA™ Kit (4387406, ThermoFisher Scientific). Next, the cDNA was preamplified 14 fold using SsoAdvanced™ PreAmp Supermix (172-5160, BioRad) with prevalidated primers purchased from BioRad (Table S13). Real-time quantitative PCR reactions were performed with the above mentioned primers and SsoAdvanced™ Universal SYBR® Green Supermix (1725271, BioRad) on a QuantStudio 3 Real-Time PCR System (ThermoFisher Scientific). All assays were performed according to manufacturer's protocols. qPCR results were analyzed using the 2^(-ΔCq)-method with three endogen genes as reference (B2M, GAPDH and RPL13A).

Demethylation of Foxp3

The quantification of Foxp3 intron 1 demethylation is based on a method defined in this publication[73]. Briefly, 10000 cells were sorted and DNA extracted using EpiTect Fast DNA Bisulfite Kit (59824, Qiagen). Bisulfite DNA was amplified using this two primers (antisense: GGTTTGTATTTGGGTTTTGTTGTTA and sens: ACCCATATCACCCCACCTAAA) following by a real-time qPCR amplification of total and demethylated *FOXP3i1* sequences using: sense primer 5'-AAACCTACTACAAAACAAAACAAC-3', antisense primer 5'-GGAGGAAGAGAAGAGGGTA-3' and Taqman probe 5'-CCTATAAAATAAAATATCTACCCTC-3' for total (demethylated + methylated) *FOXP3i1* sequences; sense primer 5'-TCTACCCTCTTCTCTTCCTCCA-3', antisense primer 5'-GATTTTTTTGTTATTGATGTTATGGT-3' and Taqman probe 5'-AAACCCAACACATCCAACCA-3' for demethylated *FOXP3i1* sequences. The ratio gives the frequency of demethylated Foxp3 gene.

Supplemental Tables

Noël *et al*.

Supplemental Table 1

Breast cancer patient's clinical parameters

Clinical parameters \ BC subtype		LumA	LumB	HER2+			TN
				All	HR+	HR-	
	No of patients: 168	82(49%)	36 (21%)	26 (16%)	18 (11%)	8 (5%)	24 (14%)
Age							
< 50 yr	35 (21%)	16 (20 %)	7 (19 %)	10 (38%)	10 (55 %)	0	2 (8%)
> 50 yr	133 (79%)	66 (80%)	29 (81%)	16 (62%)	8 (45%)	8 (100%)	22 (92%)
Menopausal status							
yes	124 (74%)	61 (74%)	27 (75%)	15 (57%)	7 (39%)	8 (100%)	21 (88%)
no	44 (26%)	21 (26%)	9 (25%)	11 (43%)	11 (61%)	0	3 (12%)
Histotype[b]							
Ductal	168 (100%)	82 (100%)	36 (100%)	26 (100%)	18 (100%)	8 (100%)	24 (100%)
Grade							
I	18 (11%)	18 (22%)	0	0	0	0	0
II-III	150 (89%)	64 (78%)	36 (100%)	26 (100%)	18 (100%)	8 (100%)	24 (100%)
Lymphovascular invasion[c]							
yes	53 (32%)	27 (33%)	8 (22%)	2 (8%)	1 (6%)	1 (12%)	16 (67%)
no	115 (68%)	55 (67%)	28 (78%)	24 (92%)	17 (94%)	7 (88%)	8 (33%)
Ki-67 (tumor)[d]							
<15%	82 (49%)	82 (100%)	0	0	0	0	0
> 15%	86 (51%)	0	36 (100%)	26 (100%)	18 (100%)	8 (100%)	24 (100%)
Stage							
I-II	153 (91%)	75 (91%)	36 (100%)	21 (81%)	17 (94%)	4 (50%)	21 (88%)
III	15 (9%)	7 (9%)	0	5 (19%)	1 (6%)	4 (50%)	3 (12%)
DCIS presence							
yes	68 (40%)	18 (22%)	25 (69%)	19 (73%)	15 (83%)	4 (50%)	6 (25%)
no	100 (60%)	64 (78%)	11 (31%)	7 (27%)	3 (17%)	4 (50%)	18 (75%)

[a] BC subtypes scored by experienced pathologists on tumor sections cIHC stained for HR (hormonal receptor: estrogen and progesterone receptors) in conjunction with cIHC and FISH-determined HER2 amplification status.
LumA: $HR^{+}HER2^{-}$ %Ki67<15%
LumB: $HR^{+}HER2^{-}$ %Ki67≧15%
$HER2^{+}$: $HR^{-or+}HER2^{+}$
TN: $HR^{-}HER2^{-}$

[b] All tumors developed from malignant differentiation of ductal cells.

[c] Lymphovascular invasion is the infiltration of tumor cells in lymphatic or capillary vessels. This is associated with a poor prognosis and metastasis.

[d] The percentage of proliferating cells among total tumor cells.

[e] Ductal carcinoma *in situ* (DCIS) is the presence of tumor cells *in situ*.

Supplemental Table 2

Frequency of CXCR5$^+$ cells in human BC TIL and tonsils

% of CXCR5[a]	Breast Cancer (n=168)			Tonsil (n=12)		
	CD4$^+$ TIL[b]	CD8$^+$ TIL[c]	TIL-B[d]	CD4$^+$ T cells[b]	CD8$^+$ T cells[c]	B cells[d]
Minimum	0	0	42	37	2	48
25% Percentile	8	4	94	41	2	69
Median	12	8	98	53	4	86
75% Percentile	17	15	100	68	7	89
Maximum	45	41	100	80	11	94
Mean frequency (μ)[a]	14	11	94	55	5	79
Std. Deviation	8	8	11	14	3	16
Std. Error of Mean	1	1	1	4	1	5
Lower 95% CI of mean	12	9	92	46	3	69
Upper 95% CI of mean	15	12	96	64	7	88

[a] The mean frequency of CXCR5$^+$ cells (μ) within the CD4, CD8 and CD20 positive subpopulations was determined from flow cytometry data of tumor and tonsil tissue homogenates.
[b] CD4$^+$ TIL and T cell represent viable (dye negative) CD45$^+$CD3$^+$CD4$^+$ cells.
[c] CD8$^+$ TIL and T cell represent viable (dye negative) CD45$^+$CD3$^+$CD8$^+$ cells.
[d] TIL-B and B cell represent viable (dye negative) CD45$^+$CD19$^+$ cells.

Supplemental Table 3

CXCR5$^+$ TIL, TLS and TIL aggregate densities in human BC

Tumor (N=79)	CXCR5$^+$ TIL/mg tissue[a]	TLS (#/cm^2)[b]	TIL aggregate (#/cm2)[c]
Minimum	0	0	0
25% Percentile	39	0	1
Median	106	1	3
75% Percentile	208	4	7
Maximum	2694	21	80
Mean (M)	258	2	6
Std. Deviation	464	4	10
Std. Error of Mean	52	0	1
Lower 95% CI of mean	154	2	3
Upper 95% CI of mean	362	3	8

[a] The density of total CXCR5$^+$ TIL (CD45$^+$CD3$^+$CD4$^+$CXCR5$^+$ Total Tfh TIL plus CD45$^+$CD3$^+$CD8$^+$CXCR5$^+$ TIL plus CD45$^+$CD19$^+$CXCR5$^+$ TIL-B) was determined using flow cytometry to analyze fresh tumor tissues.
[b] TLS are organized TIL organized with a B cell follicle and a T cell zone. TLS are scored on dual CD3/CD20 cIHC-stained FFPE tumor sections by experienced pathologists.
[c] TIL aggregates are groups of unorganized TIL (no B cell follicle or T cell zone). Aggregates are scored on dual CD3/CD20 cIHC-stained FFPE tumor sections by experienced pathologists.

Supplemental Table 4

Treg and Tfr TIL frequencies in $CXCR5^{-}CD4^{+}$ and total Tfh TIL

Tumor (n=152)	Treg in $CD4+CXCR5^{-}$ TIL (%)[a]	Tfr in total Tfh TIL (%)[b]
Minimum	2	3
25% Percentile	11	10
Median	18	15
75% Percentile	23	21
Maximum	65	71
Mean (M)	19	18
Std. Deviation	10	13
Std. Error of Mean	1	1
Lower 95% CI of mean	17	16
Upper 95% CI of mean	21	20

[a] Frequency of $CD25^{+}$ Treg in $CD4^{+}CXCR5^{-}$ TIL determined using flow cytometry.
[b] Frequency of $CD25^{+}$ Tfr in total Tfh TIL ($CD4^{+}CXCR5^{+}$) determined using flow cytometry.

Supplemental Table 5

Immunophenotype of the subpopulations in Table I

Follicular CD4$^+$ TIL infiltrating breast cancer (TIL)					
Marker	Tfh TIL			Tfr TIL	
	non-functional[a]	functional[a]	TfhX13	non-functional[b]	functional[b]
CD3	+	+	+	+	+
CD4	+	+	+	+	+
CD8	-	-	-	-	-
CD19	-	-	-	-	-
CD25	-	-	-	int	hi
CD45	+	+	+	+	+
CD45RO[c]	+	+	+	+	+
CD56	-	-	-	-	-
CXCR5	+	+	-	+	+
PD-1	lo/int	hi	hi	lo	int
ICOS	lo	int	int	lo	hi
Foxp3	-	-	-	+	+
GARP	-	-	-	-	+
CXCL13	-	±	+	-	-

[a] Based on results from the *in vitro* Tfh functional assay, which was used to evaluate activity.
[b] Based on functional tests of Tfr from tonsils (insufficient Tfr TIL from BC were available for this assay).

Follicular CD4$^+$ T cells in Tonsils (TON)				
Marker	Tfh TON		Tfr TON	
	functional[a]	TfhX13	non-functional[d]	functional[d]
CD3	+	+	+	+
CD4	+	+	+	+
CD8	-	-	-	-
CD19	-	-	-	-
CD25	-	-	+	+
CD45	+	+	+	+
CD45RO[c]	+	+	+	+
CD56	-	-	-	-
CXCR5	+	hi	+	+
PD-1	heterogeneous	hi	hi	int
ICOS	lo/int	int	int	int
Foxp3	-	-	-	+
GARP	-	-	-	+
CXCL13	int	hi	-	-

[c] Some populations of transitional TIL are detectable but not CD45RA$^+$ TIL.
[d] Based on results from that *in vitro* Tfh functional assay that evaluate their activities.

Supplemental Table 5 (cont)

Other TIL infiltrating Breast Cancer in this study						
Marker	$CD4^+$ TIL		$CD8^+$ TIL			TIL-B
	$CD4^+$ Th	$CD4^+$ Treg	$CD8^+CXCR5^+$	$CD8^+CXCR5^-$	$CD8^+CXCR5^{\pm}$ $CXCL13^+$	
CD3	+	+	+	+	+	-
CD4	+	+	-	-	-	-
CD8	-	-	+	+	+	-
CD19	-	-	-	-	-	+
CD25	-	int/hi	-	-	-	-
CD45	+	+	+	+	+	+
CD45RO[c]	+	+	+	+	+	n.d.
CD56	-	-	-	-	-	-
CXCR5	-	-	+	-	±	+
PD-1	lo/int	lo/int	lo/int	lo/int	hi	-
ICOS	lo	lo/hi	lo	lo	int	-
Foxp3	-	+	-	-	-	n.d.
GARP	-	-/+	-	-	-	n.d.
CXCL13	-	-	-	-	+	n.d.

n.d = not done

Summary:

Tfh: $CD4^+CD25^-CXCR5^+$

Activated and functional **Tfh TIL**: $PD\text{-}1^{hi}ICOS^{int}$

Non-activated and non-functional **Tfh TIL**: $PD\text{-}1^{lo/int}ICOS^{lo}$

Activated and functional **Tfh Tonsils**: $PD\text{-}1^{int}ICOS^{lo/int}$

TfhX13: $CD4^+CD25^-CXCL13^+$

Activated and non-functional **TfhX13 TIL**: $CXCR5^-PD\text{-}1^{hi}ICOS^{int}$

Activated and non-functional **TfhX13 Tonsils**: $CXCR5^{hi}PD\text{-}1^{hi}ICOS^{int}$

Tfr: $CD4^+CD25^+CXCR5^+$

Activated and functional **Tfr TIL**: $PD\text{-}1^{int}ICOS^{hi}Foxp3^+GARP^+$

Non-activated and non-functional **Tfr TIL**: $PD\text{-}1^{lo}ICOS^{lo}Foxp3^+GARP^-$

Activated and functional **Tfr Tonsils**: $PD\text{-}1^{int}ICOS^{int}Foxp3^+GARP^+$

Activated and non-functional **Tfr Tonsils**: $PD\text{-}1^{hi}ICOS^{int}Foxp3^-GARP^-$

Supplemental Table 6

CXCR5 expression on $CD8^+CD25^-$ TIL subpopulations

$CD8^+CD25^-$ TIL (n=62)	$PD\text{-}1^{lo}ICOS^{lo}$		$PD\text{-}1^{int}ICOS^{lo}$		$PD\text{-}1^{hi}ICOS^{int}$	
	$CXCR5^-$ (%)[a]	$CXCR5^+$ (%)[b]	$CXCR5^-$ (%)[a]	$CXCR5^+$ (%)[b]	$CXCR5^-$ (%)[a]	$CXCR5^+$ (%)[b]
Minimum	68	2	56	2	50	0
25% Percentile	83	7	77	10	94	0
Median	88	12	84	16	97	3
75% Percentile	93	17	89	23	100	6
Maximum	978	32	98	44	100	50
Mean (M)	87	13	83	17	94	6
Std. Deviation	7.7	78	10	10	10	10
Std. Error of Mean	1	1	1	1	1	1
Lower 95% CI of mean	85	11	80	15	92	3
Upper 95% CI of mean	89	15	85	20	97	8

[a] Frequency of $CXCR5^-$ TIL in the three different subpopulations of $CD8^+CD25^-$ TIL: $PD\text{-}1^{lo}ICOS^{lo}$, $PD\text{-}1^{int}ICOS^{lo}$ and $PD\text{-}1^{hi}ICOS^{int}$.
[b] Frequency of $CXCR5^+$ TIL in the three different subpopulations of $CD8^+CD25^-$ TIL: $PD\text{-}1^{lo}ICOS^{lo}$, $PD\text{-}1^{int}ICOS^{lo}$ and $PD\text{-}1^{hi}ICOS^{int}$.

Frequencies were determined by flow cytometric analysis of fresh tumor tissue homogenates.

Supplemental Table 7

Tumor classification based on TLS (for NanoString Assay)

Groups	Tumor	PD-1$^-$Ki-67$^-$ TLS[a]	PD-1$^+$Ki-67$^-$ TLS[b]	PD-1$^+$Ki-67$^+$ TLS[c]	Total TLS
Active TLS	1	2	7	3	12
	2	0	6	8	14
	3	0	7	4	11
	4	1	1	5	7
	5	0	5	3	8
	6	0	0	5	5
	Mean (M)	0.5	4.3	4.7	9.5
Inactive TLS	1	5	0	0	5
	2	8	0	1	9
	3	7	0	0	7
	4	10	0	0	10
	5	12	0	0	12
	Mean	8.4	0	0.2	8.6
No TLS	1	0	0	0	0
	2	0	0	0	0
	3	0	0	0	0
	4	0	0	0	0
	5	0	0	0	0
	6	0	0	0	0
	Mean	0	0	0	0

[a] Number of inactive TLS with no germinal centers (no Ki67$^+$/PD-1$^+$ cells in the B cell follicle) and less than 10% PD-1$^+$/GZMB$^+$ cells in the T cell zone.
[b] Number of active TLS with no germinal centers (no Ki67$^+$/PD-1$^+$ cells in the B cell follicle) but more than 10% PD-1$^+$/GZMB$^+$ cells in the T cell zone.
[c] Number of active TLS with a germinal center (Ki67$^+$/PD-1$^+$ cells in B cell follicle) and more than 10% PD-1$^+$/GZMB$^+$ cells in the T cell zone.

TLS were scored by experienced pathologists on dual CD3/CD20 cIHC-stained FFPE tumor sections with consecutive sections dual Ki-67/PD-1 and single GZMB cIHC-stained.

Supplemental Table 8

Clinical parameters of BC patients used in survival analysis

					IHC scores[b]					
		N=	Subtype[a]		No TLS	TLS >1			Recurrence	
			TN	HER2+		All	No act	Act TLS	Yes	No
	N=	48	27	21	16	32	15	17	13	35
Subtype	TN	27			10	17	6	11	8	19
	HER2+	21			6	15	9	6	5	16
Recurrence	Yes	13	8	5	5	8	7	1		
	No	35	19	16	11	24	8	16		
Age	< 50	15	9	6	6	9	3	6	3	12
	> 50	33	18	15	10	23	12	11	10	23
Menop	Yes	32	15	17	11	21	13	8	10	22
	No	16	12	4	5	11	2	9	3	13
Grade	1	4	1	3	0	4	1	3	0	4
	2 à3	44	26	18	16	28	14	14	13	31
LVI[c]	Yes	16	9	7	7	9	6	3	7	9
	No	32	18	14	9	23	9	14	6	26
Stage	I	27	19	8	7	20	9	11	9	18
	II-III	21	8	13	9	12	6	6	4	17
DCIS[d]	Yes	26	17	9	10	16	12	4	10	16
	No	22	10	12	6	16	3	13	3	19

[a] BC subtypes scored by experienced pathologists on tumor sections cIHC stained for HR (hormonal receptor: estrogen and progesterone receptors) in conjunction with cIHC and FISH-determined HER2 amplification status.
HER2^{+}: HR$^{-\text{or}+}$HER2^{+}
TN: HR^{-}HER2^{-}

[b] TLS were scored by experienced pathologists on dual CD3/CD20 cIHC-stained FFPE tumor sections with consecutive sections dual Ki-67/PD-1 and single GZMB cIHC-stained.

[c] Lymphovascular invasion is the infiltration of tumor cells in lymphatic or capillary vessels. This is associated with a poor prognosis and metastasis.

[d] Ductal carcinoma *in situ* (DCIS) is the presence of tumor cells *in situ*.

Supplemental Table 9

Antibodies used for flow cytometry

Antibodies				
Name	Fluorescence	Company	Reference	Clone
PD-1	VB-FITC	Miltenyi	130-117-681	PD1.3.1.3
PD-1	BV421	BD Biosciences	562516	EH12.1
CXCR5	PE	ThermoFisher	12-9185-42	MU5UBEE
CD56	PEeF610	ThermoFisher	61-0567-42	CMSSB
CD25	PercPeF710	ThermoFisher	46-0257-42	CD25-4E3
CD19	PC7	ThermoFisher	25-0199-42	HIB19
ICOS	APC	ThermoFisher	17-9948-42	ISA-3
ICOS	PC7	ThermoFisher	25-9948-42	ISA-3
CD4	AF700	ThermoFisher	56-0049-42	RPA-T4
CD4	APC	ThermoFisher	17-0049-42	RPA-T4
Fixable Viability Dye	eF780	ThermoFisher	65-0865	
CD3	VioBlue	Miltenyi	130-113-133	BW264/56
CD45	VioGreen	Miltenyi	130-113-124	5B1
CD8	BV510	BD Biosciences	563919	SK1
FoxP3	PEeF610	ThermoFisher	61-4776-42	PCH101
CD45RO	FITC	Miltenyi	130-113-549	UCHL1
CD45RA	PEvio770	Miltenyi	130-113-919	T6D11
Bcl6	PercPeF710	ThermoFisher	46-9880-42	BCL-UP
CXCL13	APC	R&D Systems	IC801A	53610

Supplemental Table 10

Antibodies used for chromogenic IHC (cIHC)[a]

Primary Antibodies					
Antigen	Dilution	Company	Reference	Host	Reactivity
CD3	Pre-diluted	Agilent	IR50361-2	Rabbit	Human
CD20	Pre-diluted	Agilent	IR60461-2	Mouse	Human
CD4	Pre-diluted	BioSB	BSB5150	Rabbit	Human
FOXP3	1/100	eBioscience	14-4777-82	Mouse	Human
PD-1	1/100	Abcam	ab52587	Mouse	Human
Ki67	Pre-diluted	Agilent	IR62661-2	Mouse	Human
GZMB	Pre-diluted	Cell Marque	262R-18	Rabbit	Human

[a] The Ultra View DAB Detection kit (760-500) and Ultra View Red Detection kit (760-501) from Roche Ventana Diagnostics includes the secondary antibodies for cIHC.

Supplemental Table 2

Antibodies used for immunofluorescence (IF)

Antibodies					
Primary antibodies					
Antigen	Dilution	Company	Reference	Host	Reactivity
CD20 (IgG_{2a})	janv-50	Abcam	ab9475	Mouse	Human
CD4 (IgG_1)	janv-40	ThermoFisher	MA5-12259	Mouse	Human
CD8 (IgG_1)	NA	Dako	IR-623	Mouse	Human
CXCR5	1/500	Abcam	ab133706	Rabbit	Human
PD-1	janv-50	ThermoFisher	RM-9116-S1	Rabbit	Human
Secondary antibodies					
Color	Dilution	Company	Reference	Host	Reactivity
AlexaFluor 488	1/200	ThermoFisher	A-21131	Goat	Mouse IgG_{2a}
DyLight 550	1/200	Abcam	ab98767	Goat	Rabbit Ig
AlexaFluor 647	1/200	ThermoFisher	A-21240	Goat	Mouse IgG_1

Supplemental Table 12

Antibodies use for multiplex IHC (mIHC)

Antibodies					
Antigen	Dilution	Company	Reference	Host	Reactivity
PD-1	1/300	Cell Signaling	86163S	Rabbit	Human
Ki-67	Pre-diluted	Agilent	IR62661-2	Mouse	Human
GZMB	Pre-diluted	Cell Marque	262R-18	Rabbit	Human
ICOS	1/400	Abcam	ab224644	Rabbit	Human
CD4	1/200	Cell Marque	104R-24	Rabbit	Human
PD-1	1/300	Cell Signaling	86163S	Rabbit	Human
CD20	1/400	Abcam	ab9475	Mouse	Human
FOXP3	1/50	eBiosciences	14-4777-82	Mouse	Human
Ki-67	1/200	Agilent	M724029-2	Mouse	Human
CD8	1/600	Akoya	OP7TL4001KT	Mouse	Human
CD68	1/700	Akoya	OP7TL4001KT	Mouse	Human
CXCR5	1/700	Cell Signaling	72172S	Rabbit	Human

CD4 CD8 CD20 FOXP3 CD68 are provided in the OPAL 7 Solid Tumor Immunology Kit, Akoya, OP7TL4001KT.
Secondary antibodies used for mIHC are provided in by:

EnVision+ Single Reagents, HRP. Rabbit, K400311-2, Ready-to-use, Agilent
EnVision+ Single Reagents, HRP. Mouse, K400111-2, Ready-to-use, Agilent

Supplemental Table 13

Validated primers used for cDNA pre-amplification and qPCR (BioRad)

Target	Assay ID
B2M	qHsaCID0015347
BCL6	qHsaCID0008961
CTLA-4	qHsaCED0003794
CXCL13	qHsaCID0015592
ENTPD1 (CD39)	qHsaCID0036576
GAPDH	qHsaCED0038674
Granzyme B	qHsaCID0013766
HAVCR2 (TIM-3)	qHsaCID0014536
IFN-γ	qHsaCID0017614
IL-7R	qHsaCID0015056
IL-10	qHsaCED0003369
IL-21	qHsaCID0008071
ITGAE (CD103)	qHsaCID0006509
LAG3	qHsaCED0042600
MAF	qHsaCED0047317
RPL13A	qHsaCED0020417
SELL	qHsaCID0014796
TCF7	qHsaCED0038899